Rising and falling diapirs, shifting depocenters, and flap overturning in the Cretaceous Sopeira and Sant Gervàs subbasins (Ribagorça Basin, southern Pyrenees)

Eduard Saura[1], Lluís Ardèvol i Oró[2], Antonio Teixell[3], and Jaume Vergés[1]

[1]Group of Dynamics of the Lithosphere, Institute of Earth Sciences Jaume Almera, ICTJA-CSIC, Barcelona, Spain, [2]Geoplay Pyrenees Ltd. and Catalonia Geological Research, Tremp, Spain, [3]Departament de Geologia, Universitat Autònoma de Barcelona, Bellaterra, Spain

Abstract The halokinetic structure of inverted salt-related continental margins is frequently obliterated by compressional overprinting. The Cretaceous Sopeira and Sant Gervàs subbasins of the Ribagorça Basin (south central Pyrenees) show evidence of salt-related extensional tectonics and diapiric growth along the Iberian Margin of the Mesozoic Pyrenean rift. We present an integrated field-based tectonic-sedimentary study to reconstruct the evolution of the Ribagorça Basin system previous to, and in the early stages of, the Pyrenean orogeny. The ~4 km thick Albian-Cenomanian Sopeira minibasin infill thins toward the basin borders, especially toward the eastern, N-S trending, Llastarri salt weld. The 90° tilt to the south of the Sopeira basin bottom records the growth of the buried north dipping Sopeira listric fault from Albian to Santonian times, when it evolved as an extensional rollover associated with the Aulet salt roller. The ~3 km thick Cenomanian-Campanian succession filling the Sant Gervàs flap displays 130° bed fanning attitude from overturned Cenomanian carbonate platform strata to upright Campanian turbidite beds. The Sant Gervàs flap development since Cenomanian times was related to the fall of a large salt pillow after the main Soperia minibasin stage. Jurassic-Campanian diachronous subsidence is also observed in the adjacent Montiberri, Faiada, and Tamurcia depocenters. Correlation with the Pedraforca, Cotiella, and Basque-Cantabrian Basins along the southern Pyrenees suggests that a significant segment of the Iberian side of the Pyrenean rift experienced a gravity-driven extension from Albian to late Santonian. The Ribagorça Basin provides an excellent field analogue for presently buried salt-related structures of extended passive margins.

1. Introduction

Continental margins and rifts are characteristic scenarios for salt basins and associated halokinetic systems [*Sannemann*, 1968; *Jackson et al.*, 1990; *Cobbold and Szatmari*, 1991; *Jackson and Talbot*, 1992; *Jackson and Vendeville*, 1994]. These are frequently inverted and shortened by orogenic processes [*Letouzey et al.*, 1995; *Canérot et al.*, 2005; *Rowan and Vendeville*, 2006; *Saura et al.*, 2014]. In such cases compressional overprinting may mask halokinetic structuration and eventually the diapiric stage may become completely obliterated. Additionally, compression may trigger the following: (1) feeder squeezing, salt extrusion, and development of folds with large overturned flaps [*Brun and Fort*, 2004; *Rowan and Vendeville*, 2006; *Callot et al.*, 2012]; (2) downward salt flow into the source layer [*Dooley et al.*, 2009]; and (3) feeder welding and consequent disconnection from the source layer.

Thick deposition of Upper Triassic evaporitic successions in the Tethys realm (Figure 1) has exerted an important role during both Jurassic-Cretaceous extension and Late Cretaceous-Paleogene compression by controlling the position of tectonic detachments [*Letouzey et al.*, 1995; *Hudec and Jackson*, 2007]. Large masses of Upper Triassic evaporites crop out in most Alpine orogens, and their involvement in diapirism was already described in detail decades ago as, for example, in the External Alps [*Laubscher*, 1977], the Pyrenees [*Rios*, 1948; *Brinkmann and Lögters*, 1968], and the Betics [*Moseley et al.*, 1981]. However, these early interpretations were later often disregarded due to the popularization of thrust tectonics concepts that were extensively applied to fold-and-thrust belts worldwide since the 1980s. Hence, diapiric structures displaying complex crosscutting relationships were frequently interpreted as originated by intricate thrust geometries.

A vast amount of seismic surveys on salt-related continental margins like the Gulf of Mexico and the South Atlantic has revolutionized the salt tectonic concepts in both extensional and compressive settings. Good
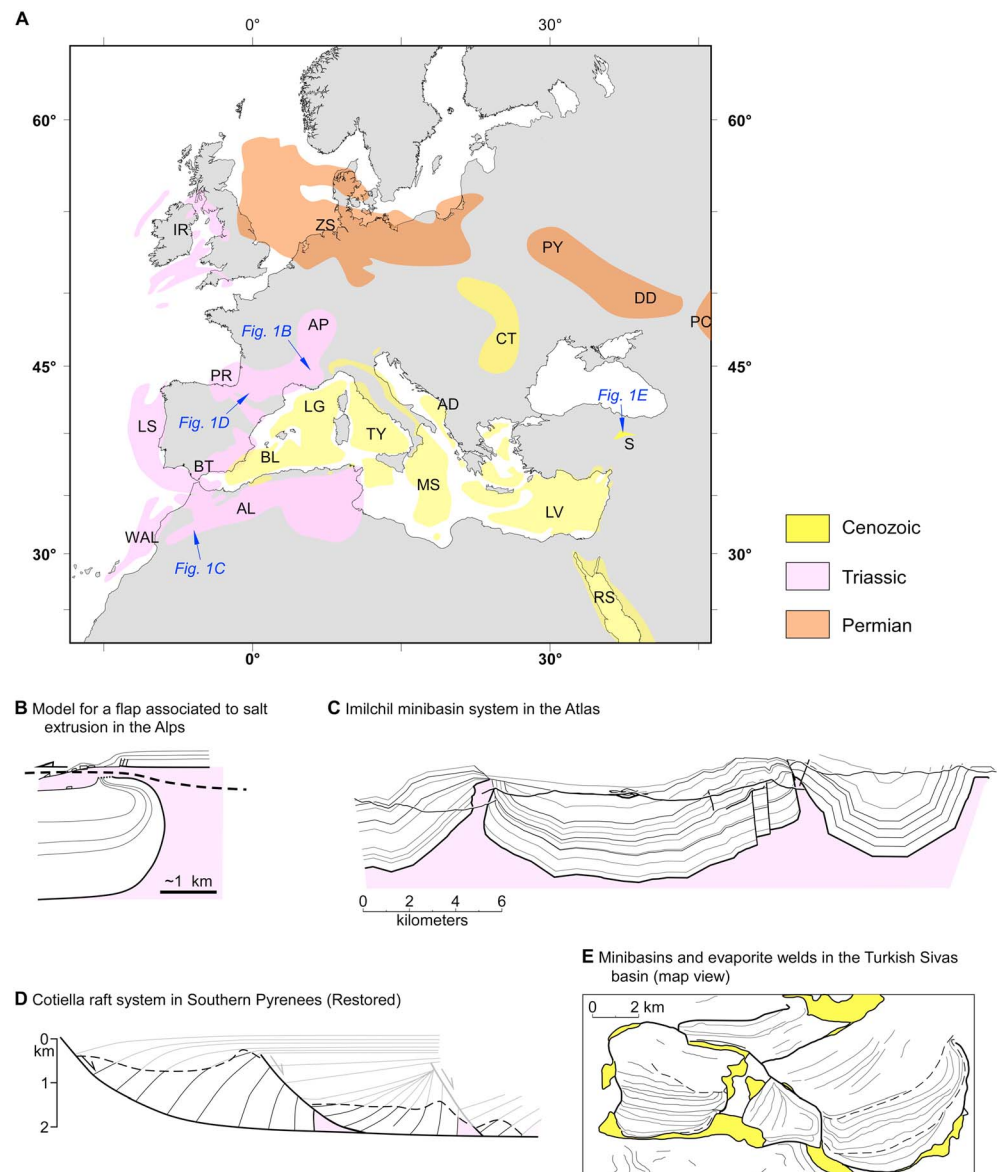
Figure 1. (a) Sketch map of western Tethys domain showing the location of the main salt basins (compiled from *Manspeizer et al.* [1989], *Shannon and Naylor* [1998], *Courel et al.* [2003], *Hudec and Jackson* [2007], *Warren* [2010], *Matias et al.* [2011], *Maystrenko et al.* [2012], and *Callot et al.* [2014]). AD = Adriatic Basin; AL = Atlas basins; AP = Alps basins; BL = Balearic Basin; BT = Betics basins; CT = Carpathian basins; DD = Dnepr-Donetz Basin; IR = Irish offshore basins; LG = Ligurian Basin; LS = Lusitanian Basin; LV = Levantine Basin; MS = Messinian Basin; PC = Pricaspian Basin; PR = Pyrenean basins; PY = Pripyat Basin, RS = Red Sea Basin; S = Sivas Basin; TY = Thyrrenian Basin; WAL = Western Atlas basins; and ZS = Zechstein Basin. Examples of salt tectonics in the western Tethys domain: (b) the Digne nappe in the Western Alps (modified from *Graham et al.* [2012]), (c) minibasin system in the Central High Atlas (modified after *Saura et al.* [2014]), (d) restored Cotiella extensional system in the southern Pyrenees (modified from *McClay et al.* [2004]), and (e) the Sivas Basin in Anatolia peninsula (modified from *Callot et al.* [2012]).

quality seismic data allow interpreting the detailed geometry of diapirs and salt-related minibasins even below allochthonous salt bodies [*Krzywiec*, 2012; *Ringenbach et al.*, 2013; *Hearon et al.*, 2014], and the structure of the upper part of continental margins dominated by listric normal faults and hanging wall rollovers and rafts was typified. These salt tectonic concepts have led to the reinterpretation of odd structures in Alpine fold belts as potential salt-related features in cases such as the Pyrenees [*McClay et al.*, 2004; *Canérot et al.*, 2005], the SW Alps [*Graham et al.*, 2012], the Central High Atlas [*Michard et al.*, 2011; *Saura et al.*, 2014], and the Sivas Basin in Turkey [*Callot et al.*, 2014] (Figure 1). Within these settings, flaps or flap folds are understood as zones of upturned strata adjacent to a diapir, resulting from arching of the diapir *roof*
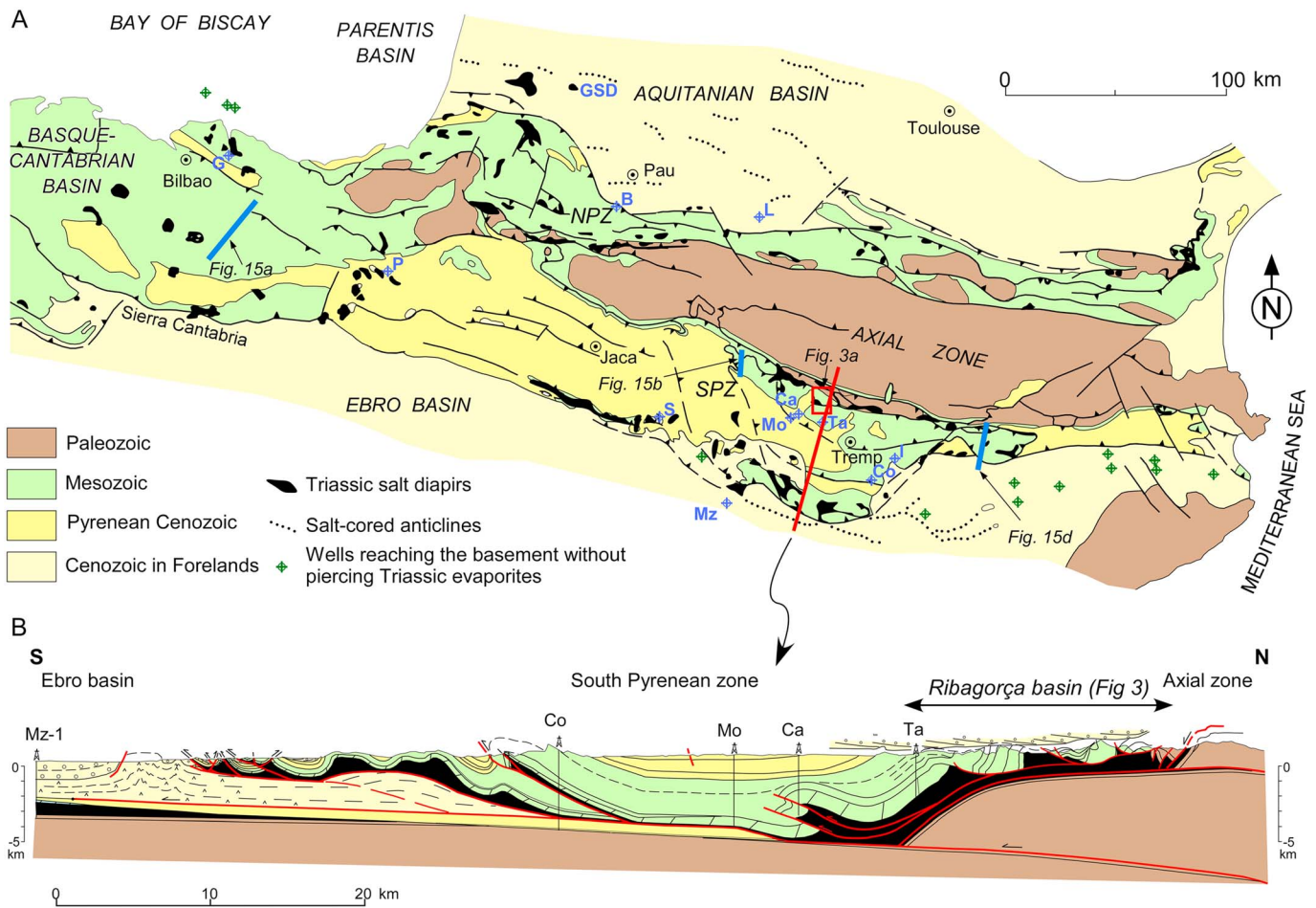
Figure 2. (a) Geological map of the Pyrenees highlighting the location of Triassic salt diapirs modified after *Teixell* [1996] and *Canérot et al.* [2005]. NPZ = North Pyrenean Zone and SPZ = South Pyrenean Zone. The red square indicates the study area. Wells and localities: B = Belair 1; Ca = Cajigar-1; Co = Comiols-1; G = Gernika-1; I = Isona-1bis; L = Lannemezan-1; Mo = Monesma-1; Mz = Monzón; P = Pamplona-4; S = Surpirenaica-1; Ta = Tamurcia-1; and GSD = Gauzacq salt dome. (b) Cross section across the South Pyrenean Zone along the Noguera Ribagorçana Valley (modified after *Teixell and Muñoz* [2000]).

above flanking strata [*Rowan et al.*, 2003; *Schultz Ela*, 2003]. They have been the subject of numerous recent studies [*Dooley et al.*, 2009; *Giles and Rowan*, 2012; *Graham et al.*, 2012; *Ringenbach et al.*, 2013; *Rowan et al.*, 2014; *Harrison and Jackson*, 2014; *Saura et al.*, 2014]. Additionally, *Alsop et al.* [2015], *Dooley et al.* [2015], and *Jackson et al.* [2015] report examples of large overturned flaps within the diapiric structures from outcrop, modeling, and seismic perspectives, respectively.

Here we present new evidence for both diapiric growth and salt-related extensional faulting along the Iberian Margin of the Cretaceous Pyrenean rift basin and for their subsequent inversion and squeezing during the Late Cretaceous-Oligocene Alpine shortening. These salt-related structures are exposed in the innermost part of the South Pyrenean thrust system, which is characterized by extensive Upper Triassic shale, marl, and evaporite outcrops and thick Jurassic to Early Cretaceous distinctive sedimentary successions that define a number of small depocenters. Structural mapping, stratigraphic section logging, and sedimentary facies analysis are used to reconstruct the evolution of two of these depocenters: the Sopeira and Sant Gervàs depocenters, which show growth strata and are immersed within a complex diapiric swarm. The migration of the sedimentary depocenters initiated during the salt-related extensional stage promptly continued during compression, together with the welding of previous diapirs and the development of a large limb overturning among other recognizable halokinetic features. These results are integrated within the larger Mesozoic Pyrenean rift basin framework that has been a topic of increased interest in the last years. In this sense, the comparison of our results with transects across the Basque-Cantabrian region [*Serrano and Martínez del Olmo*, 1990], Cotiella thrust sheet [*McClay et al.*, 2004; *Lopez-Mir et al.*, 2014a], and the Pedraforca thrust sheet [*Vergés*, 1993;

García Senz, 2002] adds to a consistent characterization of the salt-related Mesozoic Pyrenean rifting episode along the north Iberian Margin.

2. The Pyrenean Diapiric Province

The Pyrenean orogen is a branch of the Alpine belt formed between Iberia and Eurasia from Late Cretaceous to earliest Miocene times. The Pyrenean compression inverted a precursor rift, which was an E-W trending aborted branch of the Mid-Atlantic Ridge seafloor spreading that opened from the Late Jurassic to early Late Cretaceous, connecting the Atlantic and the Tethys Oceans [*Ziegler*, 1989]. A minimum shortening of 147 km has been calculated for the east central Pyrenees [*Muñoz*, 1992], which implies a restored width of >180 km between the northern and southern pinch out of the Lower Cretaceous sediments in the rift trough.

2.1. Previous Work

Halokinetic signature in the Pyrenees has long been recognized [*Rios*, 1948; *Brinkmann and Lögters*, 1968; *Wagner et al.*, 1971; *Serrano and Martínez del Olmo*, 1990; *McClay et al.*, 2004; *Canérot et al.*, 2005; *Jammes et al.*, 2010b; *Poprawski et al.*, 2014], related both to the Mesozoic extension associated to the opening of the Bay of Biscay and to the Late Cretaceous-Tertiary Pyrenean inversion, with diapir outcrops extending from the eastern Pyrenees to the Bay of Biscay (Figure 2). However, salt structures are not preserved in the Axial Zone, where the Mesozoic succession is completely eroded.

In the Basque-Cantabrian and Basque-Parentis domains, diapirism is described by several authors both off-shore [*Biteau et al.*, 2006; *Ferrer et al.*, 2008; *Roca et al.*, 2011; *Ferrer et al.*, 2012] and onshore [*Serrano and Martínez del Olmo*, 1990; *Serrano et al.*, 1994; *García-Mondéjar et al.*, 1996; *Cámara*, 1997], and coeval haloki-netic activity is reported for the onshore diapirs of the Basque-Cantabrian domain [*Gil*, 1998; *Klimowitz et al.*, 1999]. *Canérot et al.* [2005] describe examples of diapirism such as in the northern Pyrenean zone, the wes-tern Aquitanian Basin, and the western Pyrenees. In northern Atlantic Pyrenees, *Canérot et al.* [2005] date the diapiric structures to Aptian-Santonian times, although according to these authors, salt-cored anticlines already formed in the Late Jurassic, and *Biteau et al.* [2006] describe localized halokinesis during Jurassic times and more generalized along the basin edges since Barremian times.

The diapir signature in the south central Pyrenees has usually been disregarded, mainly due to the role of the salt source layer as a prominent thrust detachment level, obscuring precompressional structuration. However, raft tectonics is also reported in the western termination of this unit, in the Cotiella allochthon [*Martínez-Peña and Casas Sainz*, 2003; *McClay et al.*, 2004; *Lopez-Mir et al.*, 2014b], mainly active during the Coniacian-early Santonian. At a wider scale, *Lagabrielle et al.* [2010] propose that during the Jurassic and Early Cretaceous the Pyrenean Basin was characterized by generalized gravitational sliding of the Mesozoic cover along low-angle faults soled in Triassic salt deposits toward the center of the Pyrenean rift trough.

The source layer of all these salt structures corresponds to the Upper Triassic Keuper facies that consist of red, grey, and black shales, marls, and evaporites, mainly gypsum in outcrop, but with halite and anhydrite documented in the subsurface [*Calvet*, 1986; *Salvany*, 1990; *Flinch and Casas*, 1996; *Calvet et al.*, 2004]. The lack of a detailed characterization of compositional variations within the evaporites does not enhance to evaluate how this factor may control the behavior of this interval, as has been reported in other areas [*Butler et al.*, 2015; *Vargas-Meleza et al.*, 2015]. Keuper rocks are often intensely sheared and constitute the matrix of a tec-tonic mélange, which makes it difficult to establish the original thickness. Well and seismic data in the Bay of Biscay often portray Upper Triassic thicknesses above 1000 m [*Jammes et al.*, 2010a; *Roca et al.*, 2011], and in western Pyrenees, the Gernika-1 well drilled 1393 m of upper Triassic sediments (Figure 2) [*Lanaja et al.*, 1987], and the Pamplona-4 well drilled 422 m of Keuper rocks overlying a 521 m thick mélange with an evaporite matrix, reported as a diapir [*Lanaja et al.*, 1987]. In the Aquitanian Basin the Lannemezan-1 well found a thickness of about 2250 m (Figure 2) [*Biteau et al.*, 2006] and the Belair-1 well a thickness over 2700 m [*Infoterre-BRGM*, 2015], whereas in the Gauzacq area (Figure 2), *Canérot et al.* [2005] deduced an original Keuper thickness of about 1650 m using a restoration approach. In the south central Pyrenees, the greatest drilled Keuper thicknesses are of 1014 m in the Isona-1bis well and 895 m in the Surpirenaica-1 well (Figure 2) [*Lanaja et al.*, 1987]. Besides, several wells in the Ebro Basin (Figure 2) evidenced a sedimentary hiatus embracing the Triassic, the Jurassic, and the Early Cretaceous. In contrast, maximum thicknesses of 250 to 500 m are recorded at the surface [*Calvet*, 1986; *Salvany*, 1990; *Flinch and Casas*, 1996; *Calvet et al.*,
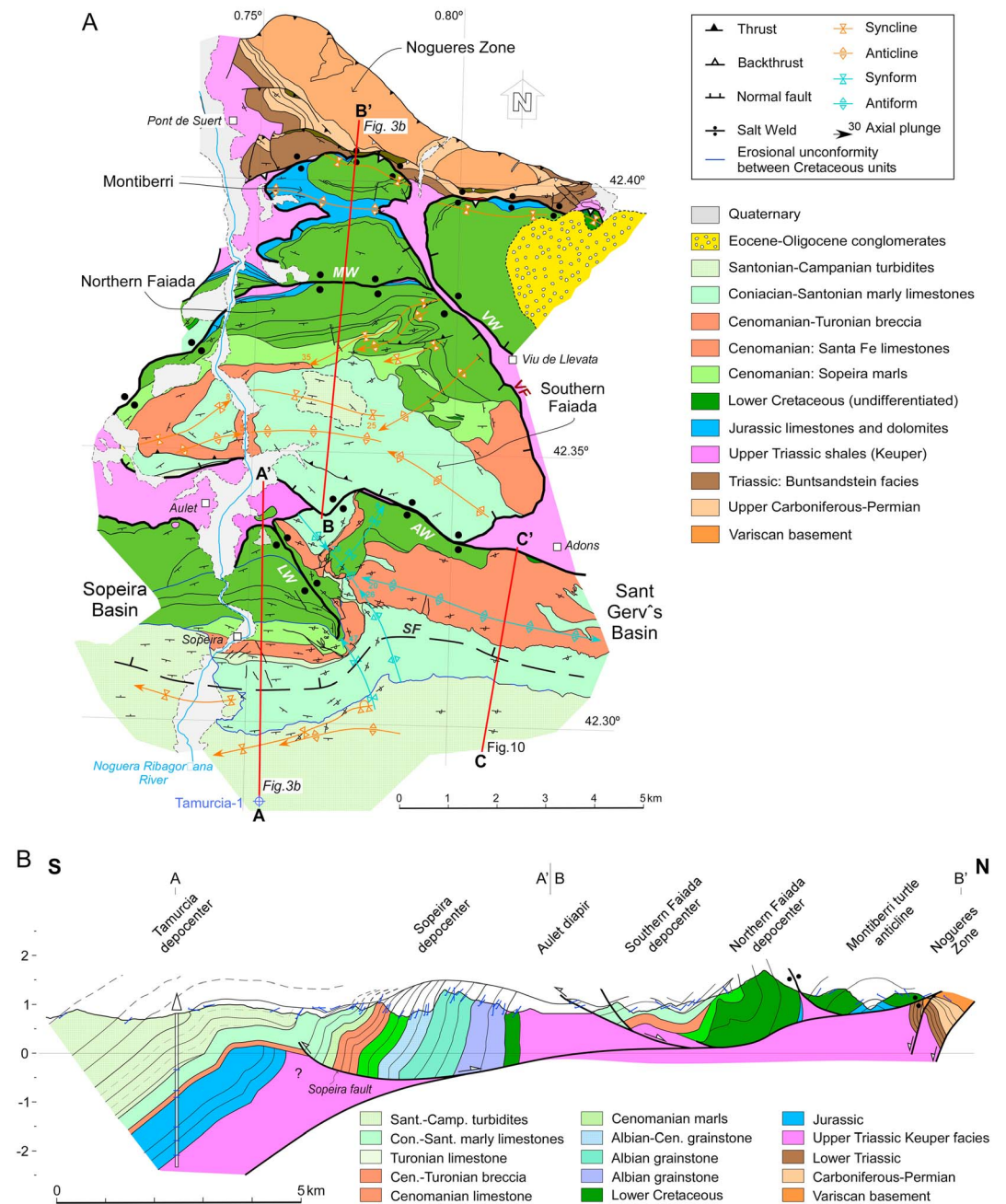
Figure 3. (a) Geological map of the Ribagorça Basin. AW = Aulet weld; LW = Llastarri weld; MW = Montiberri weld; VW = Viu weld; SF = Sopeira Fault; and VF = Viu Fault. (b) Cross section across the Sopeira, Tamurcia, Faiada, and Montiberri Basins. Note that the section extends outside the map area, 2.6 km south of the Tamurcia-1 well.

2004]. This difference may be the effect of the dissolution at surface of much of the evaporitic fraction of the original Keuper succession, as reported in the northern Pyrenean zone by *Canérot et al.* [2005].

2.2. The South Central Pyrenean Zone

The study area, the Ribagorça Basin, is located on the northern boundary of the imbricate fan of the central south Pyrenean zone (Figures 2 and 3), in contact with the basement units of the Axial Zone across a complex fault network [*Muñoz*, 1992; *Saura and Teixell*, 2000; *Teixell and Muñoz*, 2000; *Saura and Teixell*, 2006]. In the northern part of the Ribagorça Basin, the Viu Fault separates with an apparent subhorizontal attitude the Jurassic-Cretaceous succession from the underlying Keuper mass (Figure 3) [*Teixell and Muñoz*, 2000;
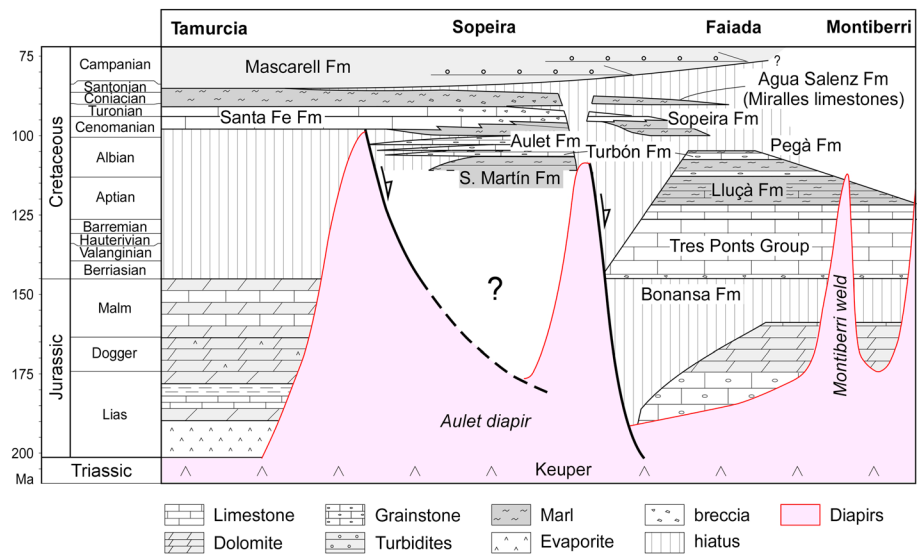
Figure 4. Chronostratigraphic panel across the Ribagorça Basin, based on field and published data [*Lanaja et al.*, 1987; *García Senz*, 2002; *Samsó et al.*, 2012a, 2012b]. The locations of the diapirs are approximate.

Saura, 2004; *García Senz and Ramirez*, 2016]. In this area, the map shows two large diapiric outcrops, the Viu de Llevata diapir in the east and the Aulet diapiric high [*Rosell*, 1967] in the west. South of these Keuper exposures a lowering of the regional structural elevation at the kilometer scale is observed, which was interpreted as the leading edge of a large basement unit at depth [*Teixell and Muñoz*, 2000] (Figure 2).

In association with salt diapirs, five main precompressive depocenters can be differentiated in the Ribagorça Basin (Figures 3 and 4). From north to south, the Montiberri depocenter is limited by the E-W Montiberri weld along its southern limit, by the NW-SE Viu weld in the east, and by the N-S Pont de Suert diapir in the west. South of the Montiberri weld, the Faiada depocenter can be divided into a northern unit and a southern unit and is bounded respectively to the west and east by the Aulet and Viu diapirs and to the south by the E-W Aulet weld. South of this diapir weld system, the Sopeira and Sant Gervàs depocenters are separated by the N-S Llastarri weld (Figure 5). South of the Sopeira depocenter, the Tamurcia-1 well drilled a succession that can be individualized from the northern successions, which we will refer to as the Tamurcia depocenter.

Several north dipping listric extensional faults are interpreted as being aligned with the E-W trending welds (Figure 3), as discussed below. Additionally, several depocenters with similar characteristics can be identified east and west of the Ribagorça Basin, which will not be analyzed in this paper.

The stratigraphic successions filling the Ribagorça Basin (Figure 4) have been dealt with in regional [*Rosell*, 1967; *Souquet*, 1967; *Garrido-Megías and Ríos*, 1972; *Drzewiecki and Simo*, 1997; *Drzewiecki and Simo*, 2000; *García Senz*, 2002] and local studies [*Caus et al.*, 1997; *Drzewiecki and Simó*, 2002]. In what follows we summarize the main sedimentary features of the area. For a synthetic account of the distribution and thicknesses of the main stratigraphic units the reader is referred to Table 1.
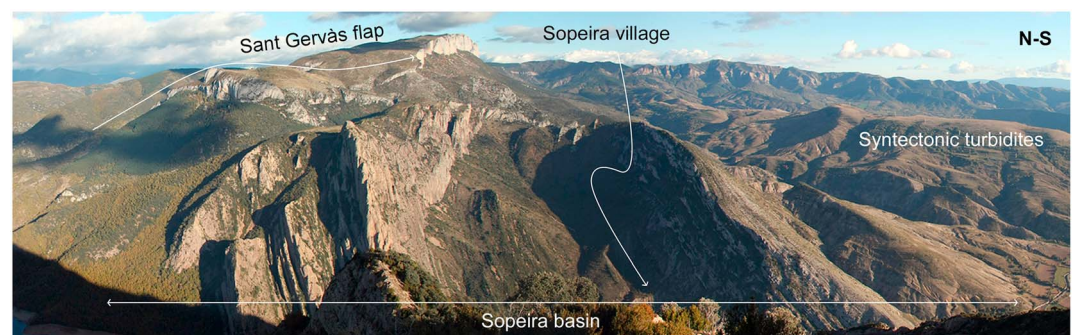
Figure 5. Panoramic view toward the east of the Sopeira (foreground) and Sant Gervàs (background) depocenters.

Table 1. Synthetic Table Illustrating the Thicknesses of the Main Formations in the Different Basins

Formation	Age	Tamurcia	Sant Gervàs	Sopeira	Faiada	Montiberri
Mascarell Formation	Santonian-middle Campanian	>1000 m	>1800 m	>300 m	>280 m	-
Agua Salenz Formation (Miralles limestones)	late Turonian-Coniacian (?)	~310 m	~1000 m	>750 m	>750 m	-
Pardina Formation	early-middle Turonian	~100 m	<20 m	~150 m	~35 m	-
Santa Fe limestones	Cenomanian-early Turonian	-	~250 m	-	~200 m	-
Santa Fe breccia	Cenomanian-early Turonian	-	-	~350 m	-	-
Sopeira Formation	early-middle Cenomanian	-	-	~425 m	~250 m	-
Aulet Formation	late Albian-early Cenomanian	-	-	~1250 m	-	-
Turbón-Pegà Formations	late Albian	-	-	~650 m		-
Sant Martín Formation	middle Albian	-	-	>300 m	>1150 m	>1000 m
Lluçà Formation	Aptian-early Albian	-	~500 m	-		
Tres Ponts Group	Berriasian-early Aptian	-	-	-		
Bonansa Formation	Jurassic	-	-	-	~90 m	~250 m
Jurassic Undifferentiated	Jurassic	~900 m	-	-	-	-

The oldest sediments filling the Ribagorça Basin correspond to limestones and dolomites with intraformational breccia of the Jurassic Bonansa Formation (Figure 4). The contact of this formation with the underlying Keuper mélange is frequently tectonized, although when observed in a stratigraphic manner, it is apparently conformable [*Samsó et al.*, 2012a]. The overlying Lower Cretaceous succession is defined by three depositional cycles [*García Senz*, 2002], mostly deposited in an extensional context. The Berriasian-Aptian cycle is formed by oolitic platform limestones (Tres Ponts Group) (Figure 4). The Aptian-middle Albian cycle is characterized by reefal limestones and marls (Lluçà Formation). Finally, the upper Albian-lower Cenomanian is made of marls and shallow marine bioclastic limestones [*García Senz*, 2002], including the upper Albian Pegà limestones and Turbón sandstones and the Albian-lower Cenomanian Serra d'Aulet grainstones [*Souquet*, 1967; *García Senz*, 2002]. The latter are particularly well exposed in the study area, where they can be separated into lower and upper parts (Figure 6). For simplicity these will be referred to as upper and Lower Aulet grainstone in this work. This system is overlain by the middle Cenomanian-Turonian cycle, which consists of carbonates displaying an east-west platform-to-basin transition, separated by a sharp erosional scarp and gravity flow deposits [*Drzewiecki and Simó*, 2002]. This cycle includes the platform limestones of the Santa Fe Formation (Figure 4), the Santa Fe breccia, the *Pithonella*-bearing Pardina limestone [*Mey et al.*, 1968; *Caus et al.*, 1993; *Drzewiecki and Simo*, 1997], and the Sopeira Formation marls, which may present an erosive base (Figures 3 and 6). The widespread Santa Fe Formation and coeval sediments were deposited during a large transgressive regime [*Rosell*, 1967; *Souquet*, 1967; *Garrido-Megías and Ríos*, 1972]. This highly expansive system is sometimes viewed as marking the rift to postrift transition in the southern Pyrenees [*Berástegui et al.*, 1990; *Vergés and García Senz*, 2001].

This platform-basin system is overlain by Coniacian-early Santonian marls and marly limestones, the Miralles limestones, with frequent slumping and megabreccia in the basal part, which represent a generalized drowning and were accumulated in a deep, gently dipping ramp [*Drzewiecki and Simó*, 2002; *Samsó et al.*, 2012b]. This unit has an erosive base and may rest on top of Cenomanian and older formations (Figure 4). The youngest Cretaceous formation of the Ribagorça Basin contains the late Santonian-Campanian siliciclastic turbidites of the Mascarell Member belonging to the Vallcarga Formation, which are highly erosive and may rest on any of the older formations [*Garrido-Megías and Ríos*, 1972]. The Mascarell turbidites are associated with the initial foreland basin development in the Pyrenees and thus have been traditionally interpreted as recording the transition from the extension to compression [*Garrido-Megías and Ríos*, 1972; *Puigdefàbregas and Souquet*, 1986].

Upper Eocene to Oligocene conglomerates deposited in isolated intermontane basins [*Rosell and Riba*, 1966, *López Olmedo et al.*, 2016]. These rocks are unconformable on folded strata of any of the previous formations.

## 3. Stratigraphy of the Sopeira and Sant Gervàs Depocenters

A record of subsidence associated to extension and to salt tectonics is exceptionally preserved in the Sopeira and Sant Gervàs depocenters (Figures 5 and 6). The two depocenters are separated at the lower terms of the Cretaceous succession by a NNW-SSE subvertical boundary, the Llastarri weld (Figure 7), associated to tight
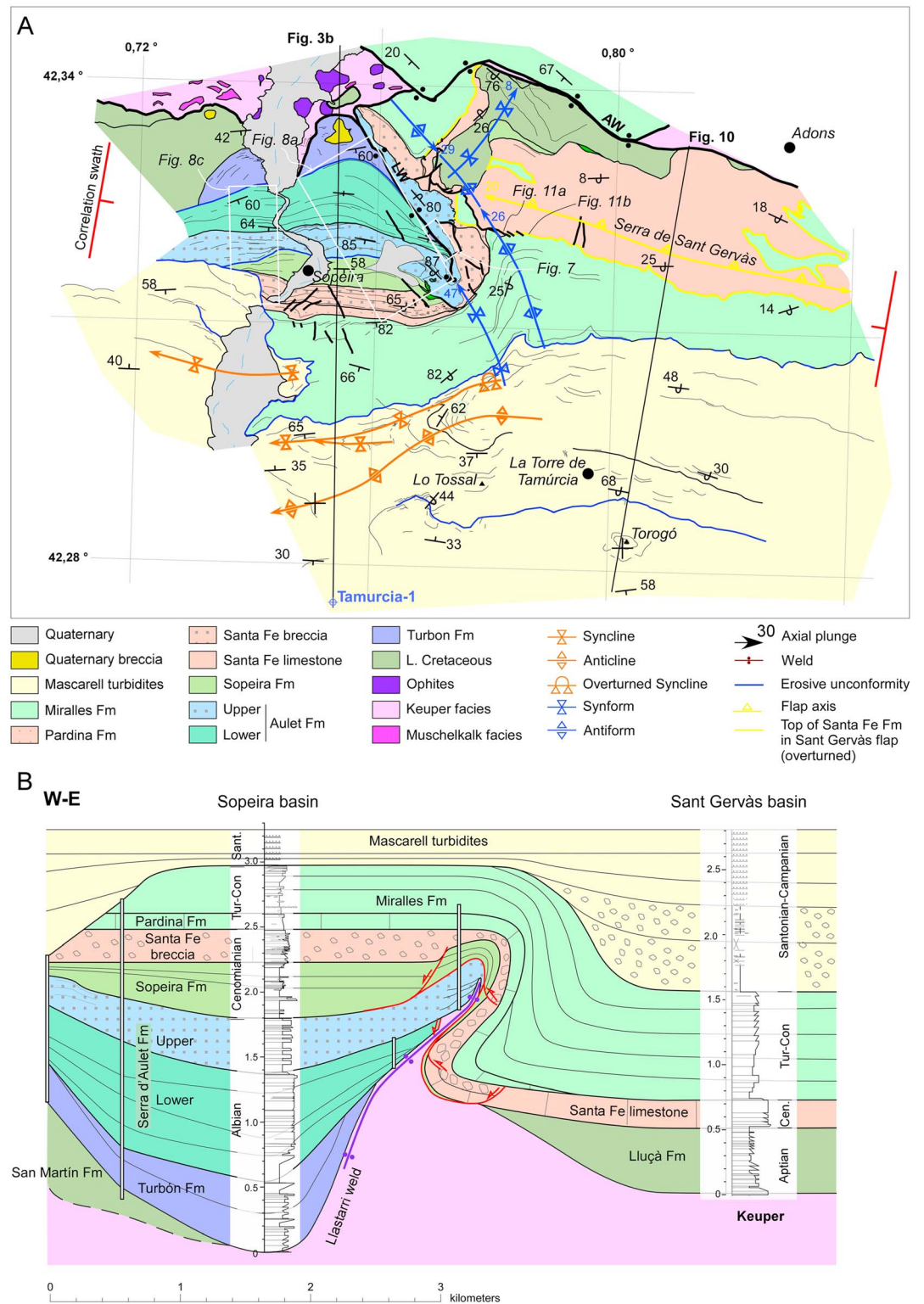
Figure 6. (a) Detailed map of the Sopeira/Sant Gervàs area. LW = Llastarri weld. AW = Aulet weld. (b) Correlation panel and depositional architecture of the Sopeira and Sant Gervàs depocenters. Most of the Albian-Cenomanian succession in the Sopeira basin correlates to a hiatus between the Lluçà and Santa Fe Formations in the Sant Gervàs depocenter. Besides, the Turonian-Campanian succession is 3 to 4 times thicker in the Sant Gervàs than in the Sopeira basin, with a thickness increase of 1500 m of the basal Mascarell turbidites.
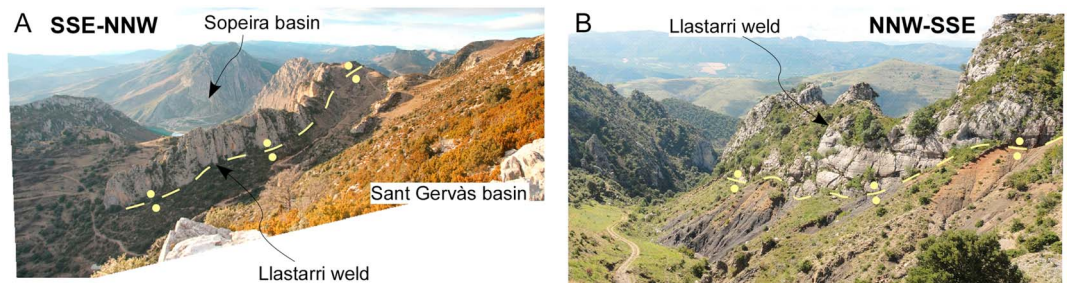
Figure 7. (a) The N-S Llastarri weld from the east. The limestone ridge corresponds to the base of the retrograding Aulet Formation clinoforms of the Sopeira basin lapping onto the former Aulet diapir. (b) Detail of the N-S Llastarri weld showing large-scale groove marks (subhorizontal) evidencing tectonic displacement between the weld walls. See Figure 6a for location.

subparallel antiforms and synforms. However, they are laterally connected as for the upper part of the Cretaceous succession (Cenomanian-Santonian) (Figure 6). This singular feature will be illustrated by detailed reconstruction of the timing relationships and the evolution of the depocenters.

The interpretation of the present-day map pattern of the Sopeira and Sant Gervàs area is not straightforward, due to the originally complex architecture and a strong compressional overprinting. The Sopeira depocenter currently displays a subvertical attitude after having undergone a rotation of ~90° along an E-W horizontal axis. Consequently, the present-day map of the Sopeira basin shows the growth geometry of the depositional sequences and their relations to the adjacent diapiric array (Figure 6).

The present-day outcrop of the Sopeira depocenter is about 4 km × 4 km and is bounded to the north by the Aulet diapir (Figures 3 and 6), along a sinusoidal map trace, reaching the southernmost position in the Noguera Ribagorçana Valley floor. The basin is filled by a 3.5 km thick Albian-Coniacian succession that is unique to it, which has been the target of several studies (Figure 8) [e.g., *Caus et al.*, 1997; *Drzewiecki and Simó*, 2002]. The infill of the Sant Gervàs depocenter, now characterized by an overturned stratigraphic polarity (Figure 9), significantly differs from that of the Sopeira depocenter due to a depositional hiatus in the Albian (Figure 6b).

The Lower Cretaceous offshore marls of the San Martín Formation [*García Senz*, 2002] characterize the lowermost sedimentary unit cropping out in contact with the Triassic evaporites of the Aulet diapir (grouped with the Lluçà Formation in the legend of Figure 6a). Their thickness is difficult to estimate due to poor exposure and internal folding but may reach several hundred meters, reducing to a few meters near the N-S Llastarri weld. Besides, the oldest sediments observed in the Sant Gervàs depocenter correspond to the Aptian-early Albian Lluçà marls formation [*García Senz*, 2002], with a maximum thickness of few hundred meters.

The basal contact of the Turbón Formation (and Pegà limestones) is sharp and punctuated by a coarse grainstone bed [*Souquet*, 1967; *García Senz*, 2002]. The Turbón Formation with a maximum of 650 m in thickness is dominated by coarsening upward parasequences of *orbitolina*-rich grainstones. Paleocurrents are east-west oriented, and the depositional bathymetry deepens westward. The Turbón Formation pinches out eastward against the N-S Llastarri weld and is truncated by the overlying strata westward as observed in the geological map (Figure 6). There is no equivalent to the Turbon depositional unit in the Sant Gervàs Basin.

The upper Albian-lower Cenomanian Aulet Formation, also referred to as Escales limestones [*Garrido-Megías and Ríos*, 1972], is composed of Orbitolina-rich grainstones [*Souquet*, 1967; *Mey et al.*, 1968], with a total thickness of about 1270 m. The Lower Aulet grainstone, with a maximum thickness of 850 m, laterally thins both westward and eastward (Figure 4), where it pinches out against the N-S Llastarri weld. The Upper Aulet grainstone with 420 m of thickness displays a depositional deepening upward trend in the central part of the basin, with a calcarenite interval at the base and finer lithologies upsequence. The Upper Aulet grainstone grades laterally into aggrading and retrograding clinoforms respectively on the western and eastern sides of the Sopeira depocenter. In the uppermost part of the succession, near the N-S Llastarri weld, the Upper Aulet succession also grades upsequence to distal facies. However, in this area large olistoliths made of proximal Lower Aulet grainstone are embedded in the formation (Figures 6, 8a, and 8b). There is no equivalent unit in the Sant Gervàs Basin.

The lower-middle Cenomanian Sopeira marls formation [*Mey et al.*, 1968] was deposited during the Cenomanian global sea level maximum, and its base records a marine flooding surface. It is formed by
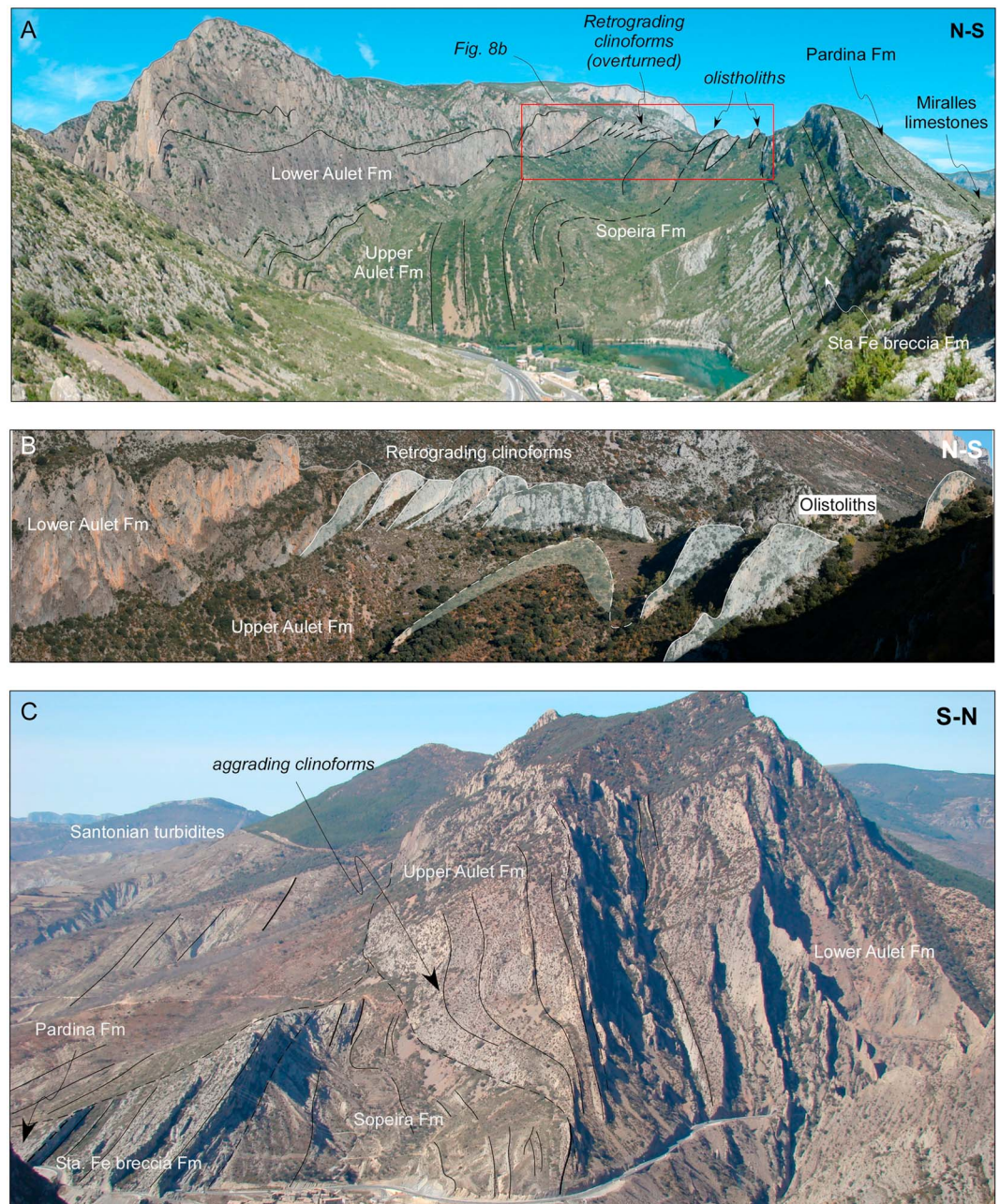
Figure 8. (a) Eastern side of the Sopeira basin. The Upper Aulet grainstone in the foreground grades to a system of retrograding clinoforms in the background. The Sopeira marls thin eastward where they interbed with a system of olistoliths made of Lower Aulet grainstone limestone. While in the foreground the succession is in upright position with decreasing dip southward, in the background the succession is mostly overturned. (b) System of retrograding clinoforms and possibly gravitational olistoliths defining the eastern margin of the Sopeira basin, attached to the N-S Llastarri weld. The view shows the subvertical to overturned top of the clinoforms, which deepen toward the left of the picture. (c) Western side of the Sopeira basin where the Albian-Cenomanian succession displays an upright attitude and an upsequence decrease of bedding dip. The Aulet Formation beds define a system of east facing aggrading clinoforms on top of which lap the beds of the Sopeira Formation that thins westward. The upper part of the succession is truncated by the Santonian Mascarell turbidites, marking the early compressional folding of this segment of the Pyrenees. See Figure 6a for location.

425 m thick interlayered nodular marly limestones and grey marls with *orbitolina* and *prealveolina* that show little variations of sedimentary facies. A deepening-shallowing upward cycle is characteristic of the Sopeira Formation [*Caus et al.*, 1997]. This marly formation thins toward the N-S Llastarri weld where it contains huge blocks (several tens of meters long and more than 10 m thick) of the underlying Aulet Formation (Figures 6,
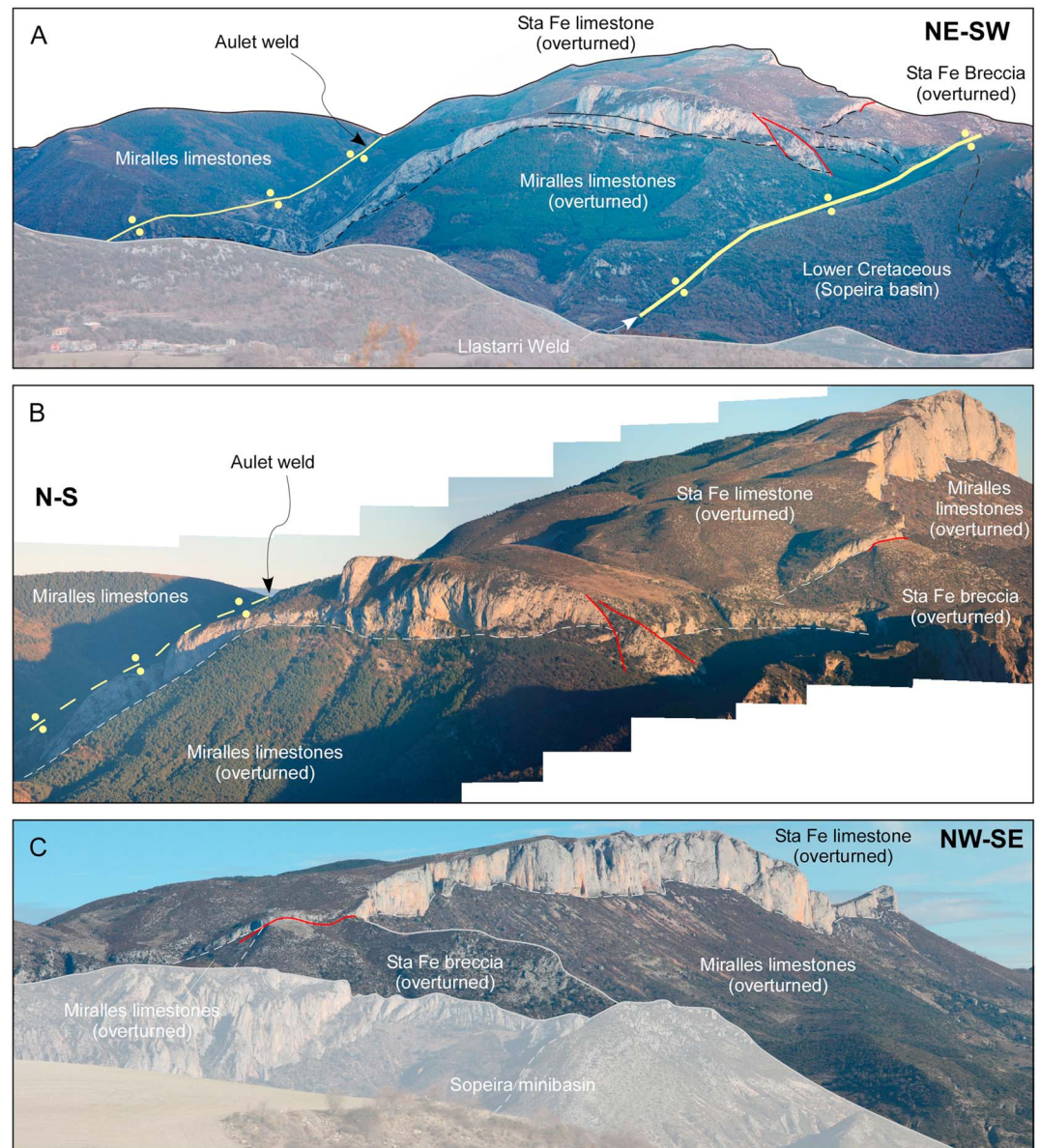
Figure 9. Western termination of the Sant Gervàs ridge showing the large overturned flap defined by the Santa Fe limestone and other formations. The Sant Gervàs flap is shown from the (a) NW, (b) west, and (c) SW. The Miralles lime-stones are exposed in the SW part of the image in an erosive window. In general, the current topography of the Sant Gervàs range east of the Llastarri weld is the actual overturned roof of the Aulet diapir.

8a, and 8b) and is truncated by the Santonian Mascarell turbidites to the west (Figures 4 and 8c). The age of the Sopeira Formation is well constrained by planktonic and Ammonites fauna [*Martínez*, 1982; *Caus et al.*, 1993; *Kennedy and Bilotte*, 2014]. The Sopeira Formation is not represented in the Sant Gervàs Basin.

The Santa Fe sequence, Cenomanian and early Turonian in age, comprises the Santa Fe limestone forma-tion [*Mey et al.*, 1968] in the Sant Gervàs depocenter and the Santa Fe breccia [*Simó and Puigdefàbregas*, 1985] in the Sopeira depocenter (Figures 4, 6, and 9). The Santa Fe breccia unit is covered by a large unconformity below the Santonian Mascarell turbidites in its western side and covers the tip point of the N-S Llastarri weld and disappears against a system of N-S faults along the western termination of the Sant Gervàs domain. The maximum thickness of the breccia is about 350 m, which decreases abruptly by a system of syndepositional faults close to the N-S Llastarri weld and finally lies below the overturned Santa Fe limestones (Figure 6). The Santa Fe breccia is composed of beds up to 25 m thick and clasts over 7 m in diameter derived from upper slope platform deposits of similar age [*Simó and Puigdefàbregas*,

1985; *Drzewiecki and Simo*, 2000; *Drzewiecki and Simó*, 2002]. The Cenomanian Santa Fe Formation with a maximum thickness of 250 m directly overlies the Aptian-early Albian Lluçà marls, in the Sant Gervàs Basin.

The *Pithonella*-bearing Pardina limestone [*Caus et al.*, 1993] commonly known as the *Pithonella* limestone [*Souquet*, 1967] is lower to middle Turonian in age [*Caus et al.*, 1993, 1997; *Drzewiecki and Simó*, 2002] and lies on top of the Santa Fe breccia. The Pardina limestone consists of deep water packstones with planktonic fauna. It reaches 150 m of thickness in the Sopeira depocenter where it is massive and slumped. These limestones represent a global transgression [*Caus et al.*, 1997]. In the Sant Gervàs area, the Pardina Formation is represented by a paleokarst surface or a very reduced (few tens of meters) succession [*Drzewiecki and Simo*, 1997].

The Aguas Salenz limestones, which were defined farther west by *Souquet* [1967], consist of well-bedded marly limestones with planktonic fauna and fine sand content. This unit was correlated by *Simó* [1985] and *García Senz* [2002] with the Miralles limestones in the Ribagorça Basin, which is the first formation that can be continuously traced from the Sopeira depocenter to the Sant Gervàs depocenter. This formation, encompassing the late Turonian and probably the Coniacian, exceeds 1000 m in thickness and consists of thin- and medium-bedded fine-grained sandy packstones, intercalated with marly intervals, arranged in fining upward parasequences which are tens of meters thick in a general deepening trend. In the Sopeira depocenter, the Miralles limestones display a 125 m thick breccia unit at its base, with large blocks of Cenomanian limestones of rudists that distally evolve to flysch deposits westward. These, grading to typical Aguas Salenz beds, display a large number of intraformational unconformities, slumps, and inner shelf carbonate olistoliths and thus indicate a high mobility in the source area. The Miralles rudist-rich limestones are truncated westward by the overlying Santonian Mascarell turbidites, whereas they can be traced eastward into the Sant Gervàs depocenter.

In the Sant Gervàs depocenter, the Miralles limestones are stratigraphically overlain by a ~650 m thick breccia made of blocks of up to 3 m of diameter of reefal limestones with rudists of Coniacian age within a marly matrix similar to the Miralles limestones containing upper Santonian fauna [*Garrido-Megías and Ríos*, 1972], which we attribute to the basal part of the Santonian and lower-middle Campanian Mascarell turbiditic formation. This formation was correlated to the Campo breccia by *Garrido-Megías and Ríos* [1972]. This breccia unit wedges out westward and cannot be observed at surface in the Sopeira depocenter (Figure 4).

Finally, the Mascarell turbidites of the Sant Gervàs depocenter are completed by a thick (>1800 m) succession characterized by deep water siliciclastic turbidites containing abundant limestone breccia, slumping, and internal unconformities [*Mey et al.*, 1968; *van Hoorn*, 1970; *Nagtegaal*, 1972]. The correlation of the turbidites in the Sopeira and Sant Gervàs Basins is not straightforward, although an eastward thickness increase of at least 800 m is envisaged as mostly occurring in the basal breccia unit (Figure 6b), as already reported by *Garrido-Megías and Ríos* [1972]. Internal unconformities within this unit separate domains with homogeneous bedding dip, and in the Torre de Tamurcia area a subhorizontal right way-up sequence is observed across a tight syncline. A large erosive unconformity is clearly observed in the Noguera Ribagorçana River where the upper part of the Mascarell turbidites is incised about 1000 m into older sediments (Figure 6a).

4. The Sopeira Minibasin Extensional Rollover

The geological singularity of the Sopeira minibasin was perceived back in the 1960s but was interpreted in different ways mostly due to the lack of diagnostic exposure of its tectonic structure, which was not analyzed in detail. *Souquet* [1967] proposed two domains separated by the Llastarri "decrochement" or flexure [*Rosell*, 1967; *Garrido-Megías and Ríos*, 1972]. *Caus et al.* [1997] indicated a half-graben above a north dipping low-angle fault, and *García Senz* [2002] interpreted the Sopeira basin as a half-graben bounded by the Llastarri Fault. *Drzewiecki and Simo* [2000] and *Drzewiecki and Simó* [2002] interpreted the Santa Fe breccias as being produced by syndepositional fault-related oversteepening.

As mentioned above, the ~3.5 km thick infill of the Sopeira depocenter was tilted about 90° along an E-W trending subhorizontal axis during and after its deposition (Figure 3b). The internal geometry of the Sopeira infill shows a stack of hooks and truncations along the contact with the N-S Llastarri diapir weld, which we interpret as halokinetic features (Figures 6 and 8a), and a bedding dip decrease upsequence, which we interpret as a synsedimentary rollover above a blind low-angle, north dipping extensional fault at depth, the Sopeira Fault (Figure 3b), as already proposed by *Caus et al.* [1997]. The Sopeira Fault should be located between the Sopeira basin and the Tamurcia-1 well as indicated by the different Jurassic-Lower Cretaceous
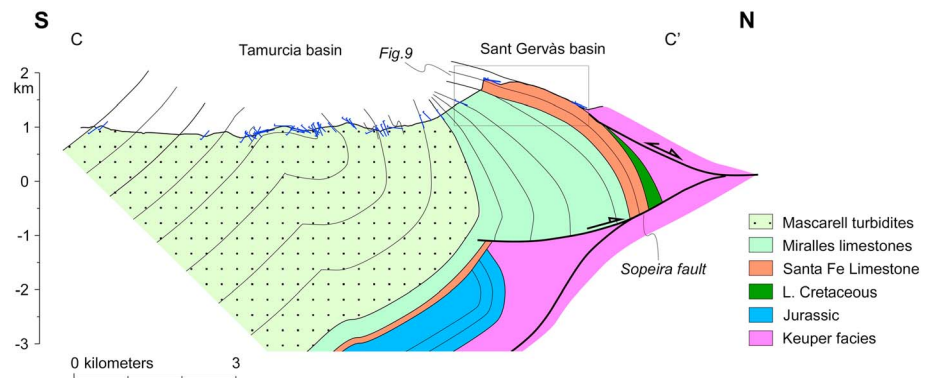
Figure 10. Cross section across the Sant Gervàs Basin. See location on Figure 3a.

stratigraphy observed in both locations, with a long depositional gap from Jurassic to the deposition of the Cenomanian in the Tamurcia-1 well. Alternatively, a progressive southward pinch out of the Lower Cretaceous succession either by wedging or truncation between both areas has been claimed [*García Senz*, 2002]. However, based on the inferences from the nearby Cotiella massif, which we discuss below, we favor the fault model. The stratigraphic differences between the Sopeira depocenter and the Tamurcia-1 well imply that the Sopeira Fault was mostly active during the Early Cretaceous, especially during Albian and Cenomanian times, when the bulk of the Sopeira minibasin infill was accumulated [*Caus et al.*, 1997]. The Sopeira Fault would run subhorizontal at depths of about 2–2.5 km with the Sopeira minibasin fill defining a rollover on its hanging wall and the Aulet high defining a salt roller or a diapir further north.

5. The Sant Gervàs Flap Structure

The Sant Gervàs flap structure is located east of the N-S Llastarri weld. The present-day exposure of the basin is characterized by a completely overturned Albian to Santonian succession, forming a ~7 km long (E-W direction), >5 km wide (N-S direction) flap, clearly marked in the field by the competent Santa Fe limestone with an overturned width of about 2 km and a subhorizontal attitude at a height of 1800 m (Figures 5, 9, and 10). The overturned flap, mostly defined by the Santa Fe limestones and, locally, by the Aptian-early Albian Lluçà marls, shows in its central part an increasing dip from south (~6° north dipping) to north (~25° north dipping). The northern boundary of the Sant Gervàs former depocenter trends ESE-WNW, subparallel or cutting the overturned succession at a very low angle. In the Adons area, where the Sant Gervàs Basin is in contact with Triassic rocks, the contact is at a constant elevation of 1300 m (Aulet weld in Figure 6). In its central part, this boundary corresponds to the Aulet weld separating the Sant Gervàs Basin from the Faiada unit. This contact drops down to 800 m in its western end. The NW boundary of the Sant Gervàs depocenter, separating it from the large Triassic outcrop of the Aulet diapir, is NE-SW oriented and cuts through the Albian-Coniacian succession, which displays a ~2 km wide, NNW-SSE trending overturned syncline (i.e., an antiformal syncline Figure 6a).

The large overturning of the limestones of the Santa Fe Formation in the Sant Gervàs range has been traditionally described as the northern flank of a large recumbent overthrust syncline [e.g., *Garrido-Megías and Ríos*, 1972; *Déramond et al.*, 1993; *García Senz*, 2002]. However, the Sant Gervàs overturned flap was not studied in detail before.

Figure 11. (a) Overturned contact between the Santa Fe limestone and the Miralles limestones showing evidence of slip. (b) Detail of the faulted contact between the Santa Fe platform and the basal Miralles breccia. See location on Figure 6a.
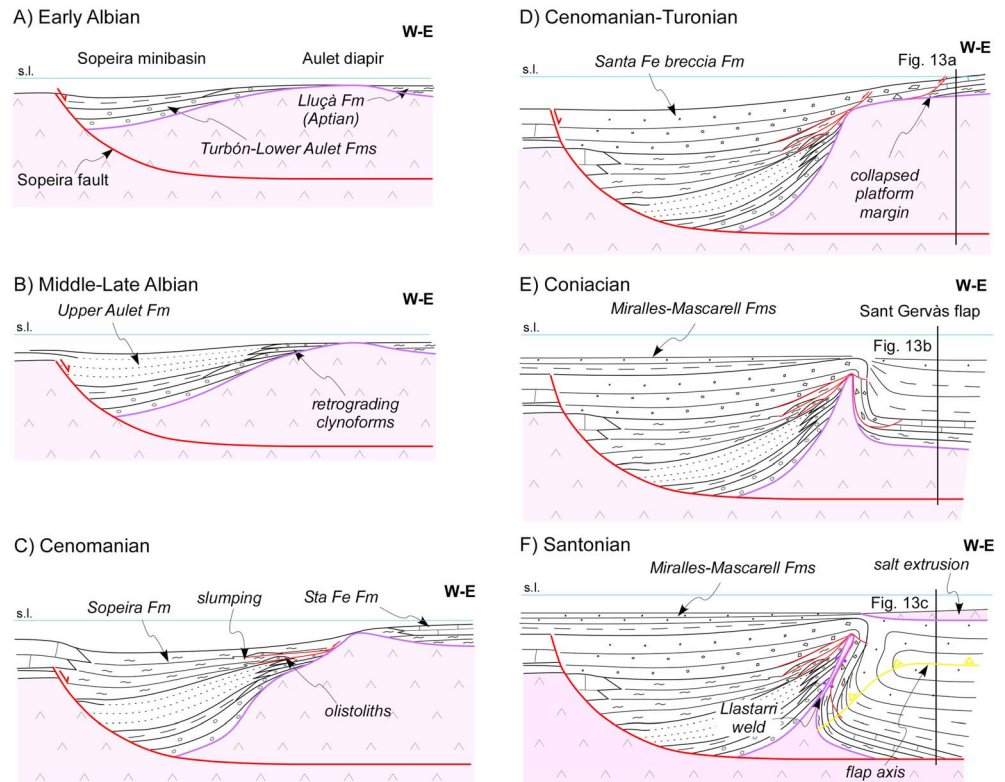
Figure 12. Synthetic evolutive model showing the shift of the main depocenter from Sopeira to Sant Gervàs depocenters at the Cenomanian-Turonian transition. From Turonian to Santonian the fall of the Aulet diapir leads to the welding of its roof and wall forming the Llastarri weld (see text for explanation).

In addition to bed overturning, the Sant Gervàs structure is characterized by a >130° bed fanning of the basin fill, from the flat-lying, overturned Cenomanian Santa Fe beds of the Sant Gervàs ridge to the upright Mascarell turbidite beds in the Torogó hill (Figure 10). The overturned panel defines a >5 km wide flap with Santonian-Campanian turbidites in the synclinal core. Angular unconformities within the overturned succession record the protracted limb rotation from Turonian to Campanian times. Additionally, the overturned contact between the Santa Fe limestones and the Miralles limestones is faulted (Figure 11a), although no major slip is envisaged along this surface. The contact between the overturned Santa Fe limestones and breccias is also sheared although both units have equivalent age (Figure 11b).

As in the Sopeira basin, the pre-Albian evolution of the Sant Gervàs depocenter is poorly constrained. The Santa Fe limestone lies on top of the black marls of the Aptian-early Albian Lluçà Formation (Figures 6 and 10), which entails a depositional hiatus encompassing the Albian and part of the Cenomanian. This depositional hiatus suggests that the Sant Gervàs area remained as a structural high during the Albian, when a thick succession was being accumulated in the Sopeira basin. The occurrence of a large flap, clearly indicative of salt tectonics [*Graham et al.*, 2012; *Rowan et al.*, 2014], requires in our view an initial southward tilt of the currently overturned succession (Figure 10), which should also have a limited thickness to allow salt to rotate and overflow it during diapir squeezing. Therefore, this suggests that the northern boundary of the Sant Gervàs depocenter was a salt pillow during the Jurassic-Early Cretaceous, aligned to the Aulet salt roller/diapir (Figure 10). Different alternatives can be envisaged for the deep structure of the Sant Gervàs depocenter. As will be discussed below, we propose that this basin is underlain by a buried extensional fault, corresponding to the eastern late propagation of the Sopeira Fault, which would be responsible for the tilting of the Sant Gervàs Basin fill during the Turonian, in combination with the uplift of the Aulet diapir. Alternatively, a stack of hooks and wedges attached to a diapir defining the southern boundary of this basin could also be considered. Subsequently, the Pyrenean contraction would result in the extrusion of the salt roller and the final stage of the development of the large Sant Gervàs flap as recorded by the fanning of the Mascarell turbidites (Figure 10).

## 6. Evolution of the Sopeira Minibasin and the Sant Gervàs Flap

The transition from Sopeira to Sant Gervàs area around the N-S Llastarri weld is extremely complex due to bed tilting and overturning and to original lateral facies variations. The upper formations of the Sopeira basin lap on the N-S Llastarri weld (Aulet grainstones, Sopeira marls, and Santa Fe breccia) and even on the overturned Santa Fe platform limestone of the Sant Gervàs unit (Santa Fe breccia) (Figures 6 and 10). The N-S Llastarri weld appears as a faulted anticlinal structure separating the Sant Gervàs and Sopeira Basins (Figure 6). This feature separates rocks that are older in the west than in the east, with different crosscutting relationships. In the west, the Albian succession of the Sopeira basin is onlapping the weld at a high angle, whereas in the east the Cenomanian succession abuts the weld at a very low angle. Additionally, the Santa Fe breccia is south dipping along the southern flank of the Sopeira depocenter, overpasses the N-S Llastarri weld, and becomes west dipping and overturned along its eastern flank (Figures 6, 8, and 11).

This varying crosscutting and geometrical relationship records a differential evolution of the Sopeira minibasin and the Sant Gervàs flap on both sides of the weld, which is illustrated along an E-W profile in Figure 12. The western limb of the N-S Llastarri weld, with tilted high-angle onlap surfaces, would correspond to the truncating diapiric wall of the Sopeira minibasin, whereas the eastern limb, with gentle onlaps, would correspond to the continuous roof of a large salt pillow (Aulet diapir in Figure 12). This implies an earlier onset of subsidence in the Sopeira minibasin (Figures 12a–12d), which later shifted eastward to the Sant Gervàs flap, producing the collapse of the diapir roof against its wall (Figures 12e and 12f). This is also consistent with a reduced to missing Jurassic-Lower Cretaceous succession along the Sant Gervàs depocenter, as discussed above.

This shift of depocenter subsidence from the Sopeira minibasin to the Sant Gervàs flap is nicely recorded both in the varying onlap relationships and the changing facies and thickness of the Albian-Turonian sequences (Figure 12). During Aptian-Albian times, the subsiding center of the Sopeira basin resulted in a westward thickening of the Turbón and Aulet Formations, associated to a general facies deepening in the same direction. In this context, the retrograding clinoforms of the Llastarri area (Figure 8a) were lapping on a N-S oriented diapir wall, the current N-S Llastarri weld, in a lentil-like manner (Figures 12a and 12b). During the Cenomanian, a regional transgression was recorded by the deposition of the Sopeira marls in the Sopeira basin and the Santa Fe limestone in the Sant Gervàs area, on top of the ~3 km thick Aulet diapir. Differential local subsidence is suggested by the large olistoliths of the Llastarri area derived from the Aulet Formation and embedded within the Sopeira marls (Figures 8a and 12c), which we interpret as having glided along the basin slope as a consequence of gravitational destabilization triggered by ongoing uplift of the large Aulet diapir (Figure 12c). The latest stages of the diapiric evolution of the Sopeira basin are recorded by the Cenomanian-Turonian Santa Fe breccia, Pardina limestone, and basal Miralles breccia. These units lap on a west dipping paleoslope, defined from west to east by the Sopeira Formation, the Aulet Formation, the Keuper rocks of the Aulet diapir, and finally, the gravitational faults cutting the Santa Fe Formation (Figure 12d).

The eastern boundary of the Sopeira minibasin can be defined as a stack of halokinetic wedges, namely, tapered composite halokinetic sequence (CHS) [*Giles and Rowan*, 2012]. These kind of stacks are characterized by broad deformation zones (>300 m) and the formation of relatively thick diapir roofs, which are progressively folded during continued diapir rise. These features imply that sedimentation rate was rapid with respect to diapir rise. Successive pulses of diapir rise are responsible for depositional thickening and deepening of sedimentary facies away from the diapir. We interpret that in the late stages of the Sopeira minibasin evolution, an acceleration of the diapir rise rate caused the failure and collapse of the diapir roof, resulting in the olistolits of the Llastarri area. This behavior is typical of most halokinetic structures because the net differential load on underlying salt increases as minibasins thicken, thereby accelerating salt flow rate, which frequently results in the development of stacked halokinetic hooks or tabular CHS [*Giles and Rowan*, 2012]. However, a clear transition to a tabular CHS is not observed in this case. This could be due to either a poor development of halokinetic hooks or the overprint of the successive stages.

A major shift in the subsidence evolution of the area occurs during Coniacian-Santonian times, when a decrease in the subsidence rate of the Sopeira minibasin contrasts with a sudden sink of the Santa Fe limestones into the Aulet diapir as recorded by the thick succession of the Miralles limestones and Vallcarga Formation into a subsiding depocenter, which show a large amount of gravitational deposits related to basin instabilities (Figure 13). During the fall of the Aulet diapir, its roof collapsed against its western wall, which eventually resulted in the closure of the Llastarri weld (Figure 12e). A short-lived but high-energy flysch deposit
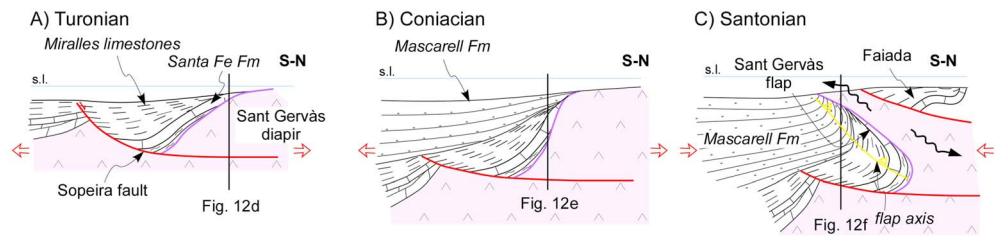
Figure 13. Synthetic evolutive N-S cross sections of the Sant Gervàs depocenter, showing the progressive verticalization and final overturning of the Sant Gervàs flap from Turonian to Santonian (see text for explanation).

with allochthonous clasts at the base of the Miralles limestones suggests a regional trigger for this change of the basin dynamics. In a N-S section, this collapse is interpreted as related to a normal fault that we propose bounds the Sant Gervàs depocenter to the south, as an eastward propagation of the older Sopeira Fault (Figure 13). The activity of this fault and the creation of a salt roller would be responsible for the migration and uplift of the Triassic rocks toward the north and the verticalization of the Santa Fe limestones.

Subsequently, the onset of compression overturned the Sant Gervàs flap (Figure 13c). With ongoing compression, a general southward tilting of the Sopeira-Sant Gervàs system around an E-W subhorizontal axis resulted in the current upturning of the Sopeira basin and overturning of the Sant Gervàs flap (Figures 3b and 10) and the welding of the E-W Aulet diapir.

The dimensions of the Sant Gervàs structure allow us to characterize it as a megaflap, understood as older strata (the Santa Fe limestone) draped along a diapir flank for a considerable vertical distance with steep (up to vertical or even overturned) dips [*Giles and Rowan*, 2012]. In this case, the rather constant thickness megaflap is onlapped by the growth wedges of the younger Sant Gervàs minibasin fill. We interpret that the Sant Gervàs megaflap as the result of the gradual steepening of the initially conformable overburden (the Santa Fe limestone) of the laterally extensive Sant Gervàs diapir top as the Sant Gervàs minibasin sank and the salt inflated, followed by overturning produced by alpine shortening. Diapir roof sinking and shortening were already envisioned by *Giles and Rowan* [2012] as the main mechanisms producing megaflaps.

7. Discussion

7.1. Structural Geometry and Tectonosedimentary Evolution of the Ribagorça Basin

The Sopeira minibasin and the Sant Gervàs flap constitute two minibasins associated to the diapiric array along the Ribagorça Basin (Figure 3). Their stratigraphic and structural characteristics differ significantly from the Faiada and Montiberri depocenters to the north; taken together, this basin system enables a wider discussion of the evolution of the northern margin of the South Pyrenean Unit during Jurassic and Cretaceous times (Figures 3 and 10). In what follows we summarize the main characteristics of the Montiberri, Faiada, and Tamurcia depocenters and integrate them in an interpretation of the whole system.

The structure of the Northern Faiada and Montiberri Basins is characterized by a shallow and flat structural contact separating Keuper rocks below from the Jurassic-Cretaceous succession above (Figure 3b) [*Saura and Teixell*, 2000; *Teixell and Muñoz*, 2000; *García Senz*, 2002]. The Jurassic-Lower Cretaceous of the Montiberri depocenter is folded into a large antiform cut by the basal contact, resembling a turtle structure anticline, characteristic of diapiric settings.

To the south, the Jurassic-Early Cretaceous succession of the Faiada depocenter is currently subvertical and welded to the north with the southern wall of the Montiberri turtle structure (Figure 3b). The synformal geometry of the Faiada Basin depicts a progressive decrease of the interlimb angle within the Cenomanian-Turonian succession. Thickness variations within these areas record southward migration of the depocenter from Jurassic to Santonian times, allowing separation of this unit into northern and southern subunits.

On its southern boundary, the Faiada Basin is bounded by the E-W Aulet thrust weld, juxtaposing the Miralles limestones in upright position to the overturned succession of the Sant Gervàs flap. This weld is interpreted as the result of the final extrusion of the Aulet diapir during the Late Cretaceous. During this process, reinjection of Triassic material toward the north, below the Faiada unit, may be in part responsible for the current change in the regional level between the Sopeira and Faiada minibasins (Figure 3b). Although not much information is
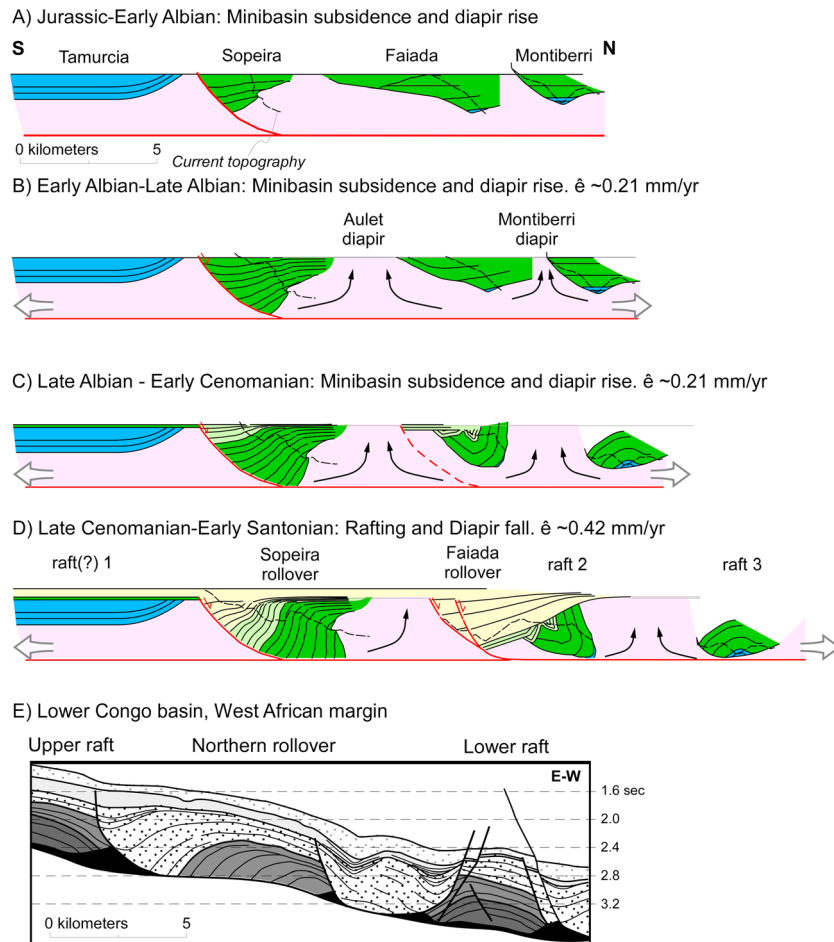
Figure 14. (a–d) Two-dimensional restoration of the evolution of Ribagorça Basin. Extension is evaluated by area balancing assuming plane strain for the Keuper (in pink) during the extension stage. Subsequent inversion of the extensional system resulted in the current configuration of the area (Figure 3a). Restored diapir widths are an approximation resulting from the homogenous distribution of the finite extension between the Aulet and Montiberri diapirs assuming there is not Triassic evaporites area loss within the section. Grounding and basal welding has been assumed for the Montiberri turtle structure. See *Lopez-Mir et al.* [2014a] for problems regarding the restoration of similar geometries. ê = extension rate. (e) Example of salt rollers related to extension detached above thin Aptian salt on the West African passive margin, Lower Congo Basin, Angola, modified after *Rouby et al.* [2002] and *Hudec and Jackson* [2007], comparable in size and geometry to the restored northern Iberian Margin.

available about the Tamurcia depocenter, the Tamurcia-1 well shows a long stratigraphic gap from the Late Jurassic to the Cenomanian Santa Fe Formation, which has a major impact on the constraints of the structural model. In addition, the succession cut by the Cajigar-1 well, located ~7.5 km south of the Tamurcia-1 well (Figure 2b), with a depositional hiatus between the Jurassic and Upper Cretaceous [*Teixell and Muñoz*, 2000; *Ardèvol et al.*, 2000], could also point to a diapiric control.

Data presented in this work picture a complex geometry for the southern margin of the Mesozoic Pyrenean rift, characterized by rafts, rollers, flaps, and minibasins separated by diapir structures which were active during the Mesozoic (Figure 14). The depocenters of the Ribagorça Basin contain different preserved thicknesses, characterized by their irregular geographic distribution. The Jurassic succession is thicker in the south (~900 m) than in the north (~250 m) and practically missing in the central part. The Lower Cretaceous succession is practically missing in the Southern Faiada, Sant Gervàs, and Tamurcia depocenters, whereas thick successions can be seen in the Montiberri (~1000 m), Northern Faiada (~1400 m), and Sopeira (>2000 m) basins. Within this interval, the Albian succession is particularly thick in the Sopeira depocenter (~1800 m), while it is much reduced in the Northern Faiada Basin (~350 m). Finally, the Cenomanian-Turonian succession is completely missing in the Montiberri and Northern Faiada Basins, relatively thick in the Southern Faiada, Sopeira, and

Tamurcia depocenters (~400–1400 m), and the thickest in the Sant Gervàs depocenter (~2300 m). These differences picture a differentiate evolution for each of the depocenters, evidencing diachroneity of the rise and fall of the different diapirs of the Ribagorça Basin.

Preserved stratigraphic successions are relatively continuous in most depocenters with the exception of the Sant Gervàs flap and the Tamurcia depocenters, which present sedimentary hiatuses at the base of the late Cenomanian. Additionally, the Montiberri Basin lacks a post-Aptian stratigraphic record and the Southern Faiada and Sopeira depocenters lack the Jurassic and part of the Lower Cretaceous at their base. Depositional continuity leads us to roughly equate sedimentary thickness and subsidence (without regarding eustatic effects) of the preserved part of the successions. In what follows, we qualitatively discuss differentiated subsidence evolution based on the stratigraphic record in each basin, assuming that missing intervals correspond to nondeposition. Alternatively, these lacking intervals could actually correspond to differential uplift and erosion, picturing an even more complex evolution of the Ribagorça Basin.

The Tamurcia-1 (for consistency with the rest of the text) well cuts through a continuous and thick Jurassic sedimentary record, whereas the Montiberri and Northern Faiada minibasins show thin and discontinuous Jurassic successions, suggesting that during the Jurassic, subsidence was mainly located in the Tamurcia depocenter and, to a lesser degree, in the Montiberri turtle structure and the Northern Faiada minibasin. We interpret these thickness variations as resulting from early diapiric activity triggered by a regional extensional regime, although further resolution within the Jurassic history cannot be obtained. This scenario was enhanced during the Early Cretaceous, when thick sedimentation was initially located in the Montiberri turtle structure and the Northern Faiada minibasin, and later shifted to the Soperia minibasin during the Albian (Figures 14a and 14b). In the Faiada minibasin, the erosional truncation of the lower Cretaceous succession by the overlying Upper Cretaceous indicates that its southern boundary was uplifted during the Albian, when subsidence was mainly focused in the Sopeira minibasin, suggesting that the Aulet diapir rose as a salt roller separating both basins (Figure 14b). It must be pointed out that the Early Cretaceous is not recorded in the Tamurcia basin farther south, as is the case for most of the South Pyrenean Unit south of this point, where the Lower Cretaceous is frequently missing or much reduced.

From the Cenomanian to early Santonian, rapid subsidence was concentrated in the Southern Faiada and Sopeira rollovers, although sedimentation was also important in the Sant Gervàs flap and the Tamurcia depocenter after the middle Cenomanian (Figure 14d). This increase in subsidence rate, especially in the Southern Faiada rollover, is associated with a twofold increase of the local extension rate. In this scenario, the Montiberri turtle structure and the Northern Faiada minibasin would have glided northward as rafts along a regional detachment defined by the northern continuation of the Sopeira Fault. Finally, after the mid-Santonian, the Pyrenean inversion uplifted the Montiberri and Faiada units and produced the extrusion of the Aulet diapir. This resulted in the final development of the Sant Gervàs flap, as recorded by the deposition of the Mascarell turbidites, mostly in the southern part of the study area, and thinning rapidly toward the north. This period probably also corresponds to the closure of the N-S Llastarri weld and the rotation along a horizontal axis of the Sopeira and Sant Gervàs Basins.

In summary, we can differentiate three main stages in the evolution of the Ribagorça Basin during preorogenic times. The initial extensional stage from the Jurassic to the early Albian is characterized by minibasin formation and diapir rise as suggested by growth geometries (Figure 14). The second stage, from the mid-Albian to the early Cenomanian, corresponds to continued minibasin subsidence (Sopeira minibasin and the lower part of the Sant Gervàs flap) and by the overlap of the northern part of the Aulet diapir at Southern Faiada. From late Cenomanian to Turonian times ongoing extensional faulting was associated to diapir fall, rollovers and rafts, and a substantial increase of the local extension rate (Figure 14). The subsequent evolution was determined by the Pyrenean tectonic inversion, which resulted in diapir welding, salt extrusion, and major diapir flank overturning (Sant Gervàs flap).

In this scenario, the current Ribagorça Basin would define the upper part of a diapiric extensional system at the Iberian Margin of the Pyrenean rift trough, with geometries and dimensions comparable to other currently buried salt-related passive margins (Figure 14d), and thus providing an interesting stratigraphic and structural field analogue. This Jurassic-Early Cretaceous extensional system would be detached along the Keuper rocks and completely decoupled from the underlying Permian-Triassic rift systems, well characterized in the Axial Zone massif [*Saura and Teixell*, 2006].
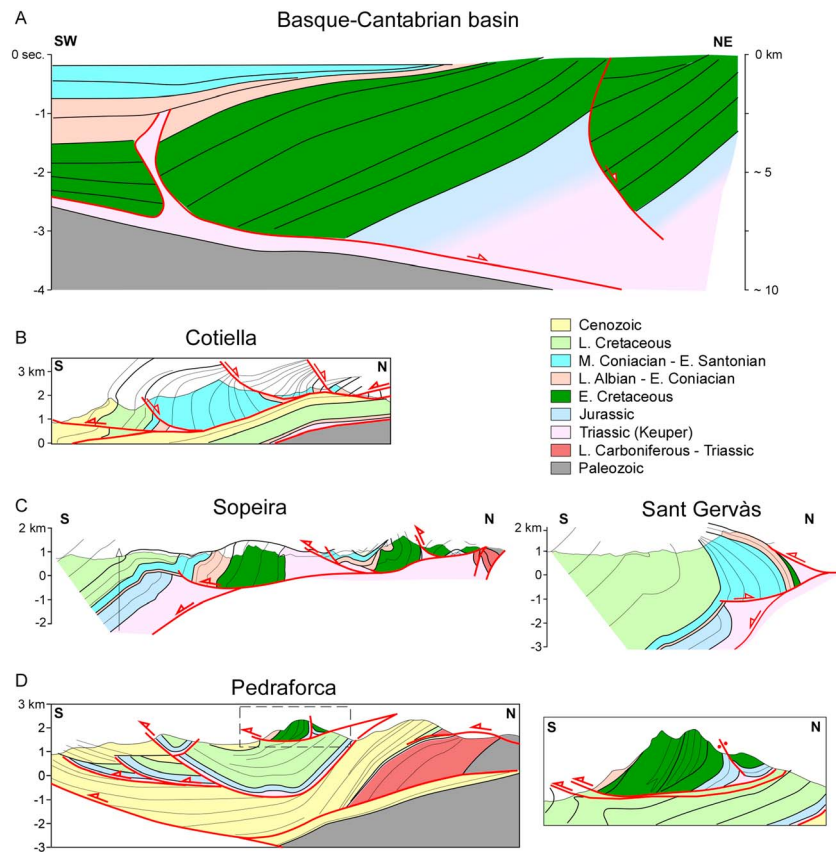
Figure 15. Cross sections across diapiric rollovers of the southern Pyrenees. All sections are at the same scale; see locations in Figure 2a. (a) Apodaca structure in the Basque-Cantabrian Basin (modified after *Serrano and Martínez del Olmo* [1990]). (b) Cotiella Massif (modified after *Lopez-Mir et al.* [2014b]). (c) Ribagorça Basin. (d) Pedraforca thrust system (modified after *Vergés* [1993]).

7.2. Large-Scale Gravity Gliding on the Northern Margin of the Iberian Plate During Mesozoic Times

A wider understanding of the evolution of the Iberian Margin of Pyrenean rifting during Mesozoic times can be achieved by comparison of four areas of the southern Pyrenean fold and thrust system: the Apodaca structure in the western Pyrenees/Basque-Cantabrian Basin, the Cotiella Massif and the Ribagorça Basin in central Pyrenees, and the Upper Pedraforca thrust sheet in eastern Pyrenees. The Cotiella and Upper Pedraforca thrust sheets show spectacular outcrops including their basal thrusts, which are buried in the case of the Apodaca structure and the Ribagorça Basin. Whereas the deep structure of the western Pyrenees/Basque-Cantabrian Basin has been imaged by multiple seismic surveys since the 1970s, there is a lack of data about deep structure of the Ribagorça Basin other than the Tamurcia-1 well.

The Apodaca structure of the western Pyrenees/Basque-Cantabrian Basin is well constrained by seismic profile S82-22, surface geology, and exploration wells [*Serrano and Martínez del Olmo*, 1990; *Infoigme*, 2015a] (Figure 15a). The ~18 km wide Apodaca structure (basin) shows a ~7.5 km thick south dipping sedimentary succession ranging from Jurassic to Santonian infilling a half-graben basin bounded by a north dipping listric extensional fault [*Serrano and Martínez del Olmo*, 1990]. The south dipping internal arrangement of the bedding in the hanging wall is interpreted as a rollover, linked with the activity of the normal fault, detached along the Upper Triassic evaporites, and associated with a diapiric structure on its footwall [*Serrano and Martínez del Olmo*, 1990]. The fault is aligned to currently outcropping diapirs, exposing Upper Triassic evaporites, which suggests an interrelated evolution. Immediately north of this lineament, E-W migration of the Mesozoic depocenters is evident in seismic data [*Infoigme*, 2015b]. The Pyrenean compression transported to the south the extensional diapiric system on top of the Ebro foreland basin along a major basal thrust detached along the Upper Triassic evaporites, breaching the surface in the Sierra de Cantabria

(Figure 2). The subhorizontal attitude of the youngest precompressional deposits suggests that compression did not significantly modify the internal extensional geometry of this unit (Figure 15a).

The Cotiella Massif is an allochthonous thrust sheet constituted by several units exposing middle Coniacian-lower Santonian strata with particular geometric relationships (Figure 15b). Extensional deformation within the Cotiella Massif was first described by *Séguret* [1972] and lately interpreted as a gravity-driven extensional system developed in the Bay of Biscay-Pyrenean paleorift margin of the Atlantic Ocean [*McClay et al.*, 2004; *Lopez-Mir et al.*, 2014b]. The subsequent Pyrenean contractional deformation detached the whole system along the Keuper rocks, emplacing it about 12 km southward on top of Eocene sediments along a very low angle footwall ramp, without significantly modifying the extensional structure [*Lopez-Mir et al.*, 2014b].

The current configuration of the Cotiella Massif illustrates a system of extensional basins bounded by north directed listric faults and filled by middle Coniacian-early Santonian sediments depicting large rollover geometries. According to *Lopez-Mir et al.* [2014b], the formation of these geometries is the combination of post-rift gravitational collapse triggering fault formation and passive diapirism and followed by subsequent welding of the diapiric structures during the compressional stage. Additionally, E-W depocenter migration associated to N-S structures is also reported in this area [*Lopez-Mir et al.*, 2014b].

The Pedraforca unit is an allochthonous thrust system, which can be divided into the Upper and Lower Pedraforca thrust sheets (Figure 15d). The Lower Pedraforca thrust sheet was emplaced 27.4 km to the south during the early-middle Eocene [*Vergés*, 1993], carrying on its back the Upper Pedraforca thrust sheet emplaced during the latest Cretaceous-Paleocene [*Vergés et al.*, 1995]. The Upper Pedraforca thrust sheet is composed of thick Jurassic to Late Cretaceous subvertical stratigraphic units above a syncline-like folded basal thrust. The footwall is composed by a younger stratigraphy, mostly Upper Cretaceous, which gently dips toward the south, and is cut at low angle by the Upper Pedraforca basal thrust. The Upper Pedraforca thrust sheet was interpreted as the hanging wall of high-angle and north dipping Jurassic-Early Cretaceous normal fault [*Vergés and Martinez*, 1988; *Vergés*, 1993; *García Senz*, 2002], although in our opinion it could be reinterpreted as a roller.

The above described characteristics can be integrated into the wider framework of the northern Iberian Mesozoic margin characterized by an intricate network of diachronic depocenters, showing migration of the subsidence both along and across this margin. These depocenters were presumably bounded by diapiric features aligned approximately N-S and E-W, which suggests a polygonal array typical of diapiric provinces such as the Gulf of Mexico or the Flinders Ranges in Australia. The age of the sediments filling these depocenters ranges from Jurassic to Santonian, whereas younger sediments seem to overlap and fossilize most of these features. North dipping listric faults frequently bound to the south of these basins, which are associated to rafts and rollover geometries on their hanging walls and to salt rollers and diapirs on their footwalls. This diapiric system defined a large gravity-driven extensional margin detached along the Keuper rocks and deepening toward the north from Cenomanian to late Santonian. The latter inversion of the whole margin during the Pyrenean orogeny brought the whole extensional system southward on top of the Ebro foreland basin, also detached along the Keuper rocks. Contraction is mainly recorded by squeezing and welding of the diapiric structures and locally by verticalization of the stratigraphic successions.

In this scenario, the time span recorded by the infill of the basins of the Ribagorça Basin allows a more accurate timing of the diapiric stage than previously known for the tectonic evolution of the Mesozoic Pyrenean margins. Although the main diapiric activity probably started during the Aptian-Albian [e.g., *Canérot et al.*, 2005; *Roca et al.*, 2011], older Jurassic-Early Cretaceous anticlinal structures on the northern Pyrenees are interpreted as a consequence of punctuated periods of basin inversion by *Canérot et al.* [2005]. The irregular distribution and the thickness variations of the Jurassic among the Ribagorça Basin minibasins could actually be recording the coeval onset of salt tectonics, also in the southern Pyrenees. However, the major change in the evolution of the Iberian continental margin seems to be recorded by the changing diapiric geometries of the Montiberri turtle structure and Northern Faiada minibasin, filled by Jurassic-Lower Cretaceous deposits, and the Southern Faiada, Sopeira, and Sant Gervàs depocenters, filled by Albian-Santonian deposits. This suggests that the early stages of the Pyrenean diapiric province were mainly characterized by minibasin formation and salt withdrawal, whereas the successive stages were characterized by gravity gliding along listric faults as clearly evidenced by *Lopez-Mir et al.* [2014b] in the Cotiella area. During this stage, the Jurassic-Early Cretaceous minibasins would have glided as rafts toward the deeper parts of the basin. These units, clearly
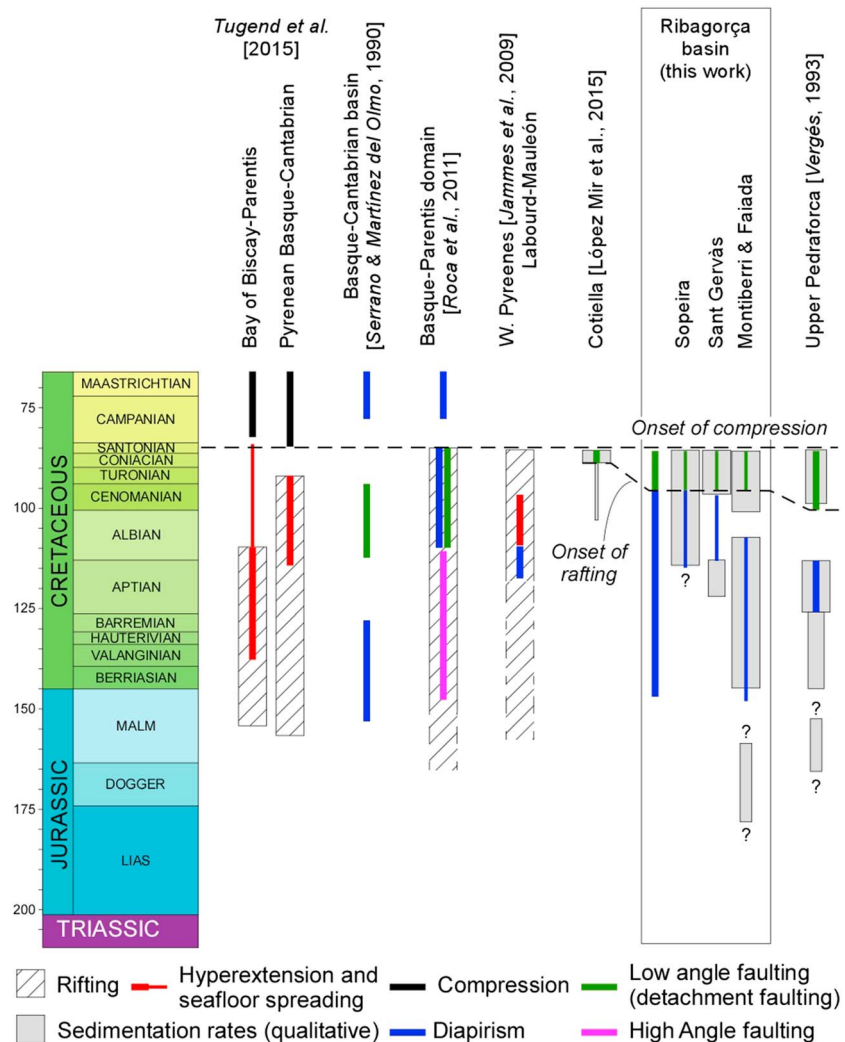
Figure 16. Compilation of the main tectonic events occurring in the Pyrenean domain according to different authors. On the right-hand side, the ages of the sediments filling the structures illustrated in Figure 15 are plotted. Variations in bar width illustrate the qualitative evolution of the sedimentation rate for each structure.

exposed in the Serra Faiada and Montiberri Basins, would currently be eroded in the innermost parts of the Pyrenean orogen in other areas, such as the Cotiella and Pedraforca transects for example. Minibasin development associated with raft tectonics, whose onset progressively migrated westward (Figure 16), went on up to the late Santonian, when compression started, as recorded by the regional unconformity at the base of the Vallcarga turbidites [*Puigdefàbregas et al.*, 1992]. Their deposition seems to be controlled by the first Pyrenean thrust sheets (Bóixols and Nogueres units). However, they are markedly controlled by the previous diapiric basin architecture and the development of the Sant Gervàs flap. In this sense, it must be highlighted that the main development of the Sant Gervàs flap is another argument supporting the onset of compression during the Santonian. Our proposed timing is roughly in agreement with that proposed by *Serrano and Martínez del Olmo* [1990] (Figure 16).

As for the deep compressional geometry, which is not the main aim of this work, both the Cotiella and the Pedraforca thrust sheets are useful to constrain the potential geometry of the Ribagorça Basin extensional system. We infer the deeper part of the cross section as a positive reactivation of the extensional system above a basal thrust (never observed).

The changing dynamics of the diapiric system can also be correlated with large-scale models for the evolution of the Mesozoic Pyrenean margins [*Serrano and Martínez del Olmo*, 1990; *Jammes et al.*, 2009; *Roca et al.*, 2011]

(Figure 16). *Roca et al.* [2011] differentiate two stages during the extensional stage in the Basque-Parentis domain (Figures 2 and 16). The initial stage, pre–mid-Albian in age, is characterized by high-angle extensional faulting, whereas the younger stage, from mid-Albian to Santonian, is characterized by low-angle (detachment) extensional folding and associated diapirism. According to *Jammes et al.* [2009], *Lagabrielle et al.* [2010], and *Tugend et al.* [2015], the initial part of the latter stage also corresponds to hyperextension and mantle exhumation in the Bay of Biscay-Parentis domain and the western Pyrenees. These stages are in agreement with the changing dynamics of the diapiric system in the Ribagorça Basin (Figure 14). The initial Jurassic-early Albian stage would correspond to the main development of the Montiberri and Northern Faiada depocenters and the initial stages of the Sopeira depocenter, whereas the early Albian-Santonian stage would correspond to the main development of the Sopeira depocenter and specially the Sant Gervàs and Cotiella Basins, associated with north directed listric faults and a sudden increase of the sedimentation rate and extensional gliding after the late Cenomanian (Figure 16).

8. Conclusions

A system of thick diachronous sedimentary depocenters immersed in a diapiric swarm defined by principal E-W and secondary N-S trending diapirs is interpreted in this work as part of a large diapiric province along the Iberian Margin of the Pyrenean rift. The Jurassic-Cretaceous successions filling the Sopeira, Sant Gervàs, Montiberri, and Faiada depocenters of the Ribagorça Basin in the southern Pyrenees show significant thickness variations and a large number of halokinetic features successively obliterated by a gravity-driven extensional event up to late Santonian and subsequent compression.

The 4 km wide by ~4 km thick Sopeira minibasin is characterized by a significant wedging of its Albian-Cenomanian infill toward the basin borders, especially toward the N-S trending Llastarri salt weld, where it wedges out by onlap, sedimentary truncation, and faulting. A general depositional deepening from small carbonate platforms attached to the Llastarri weld to basinal marls in the center of the basin characterizes the evolution of the minibasin linked to salt diapir growth. The 90° tilt to the south of the Sopeira minibasin fill is partly interpreted as recording the growth of a north dipping listric fault, the Sopeira Fault, buried at depths of about 2–3 km. The Sopeira minibasin evolved as an extensional rollover, and the Aulet diapir became a salt roller from late Cenomanian to late Santonian times. Subsequently, the Pyrenean compression finalized the verticalization of the minibasin fill.

The 7 km wide (E-W direction) and 5 km long Sant Gervàs flap is defined by a ~3 km thick Cenomanian-Campanian succession displaying a 130° bed fanning attitude from overturned Cenomanian beds of the former basin bottom to upright Campanian turbidite beds. The spectacular Sant Gervàs flap is clearly defined in the field by the competent Santa Fe limestone, which has been overturned to a subhorizontal position at an altitude of ~1800 m. The flap development is recorded by the accumulation of the Cenomanian-Campanian succession, as recorded by the multiple angular unconformities.

The onset during Cenomanian times of the Sant Gervàs flap growth as a southward tilted panel is nterpreted as related to the fall of a large salt pillow. Thick breccia units, composed by Cenomanian platform clasts, were shed into the neighboring Sopeira subbasin fossilizing the N-S Llastarri diapiric growth. Subsequently, the Sant Gervàs flap further tilted southward as a rollover in the hanging wall of an inferred north dipping extensional fault at depth in continuity with the adjacent Sopeira Fault. The overturning of the salt-related flap structure progressively occurred after the late Santonian during the Pyrenean compression.

The northward extensional glide of the Soperia, Sant Gervàs, Montiberri, and Faiada diachronous depocenters is also recognizable in the Upper Pedraforca, Cotiella, and northern Basque-Cantabrian Basins. Despite local diachroneity, this suggests that a significant portion of the Iberian Margin of the Pyrenean rift trough was involved in a gravity-driven extensional stage at least from late Albian to late Santonian, which occurred at the end or closely after the crustal hyperextension proposed along the western Pyrenean Basin. This stage briefly preceded the onset of Pyrenean shortening at the end of Santonian time, when tectonic inversion obliterated much of the previous extensional structure.

The dimensions and characteristics of the well-exposed Ribagorça Basin on the upper part of the extensional diapiric system of the Iberian Margin of the Pyrenean rift, which evolved through diapiric and extensional

processes during the Cretaceous, are comparable to other currently buried salt-related and extended passive margins elsewhere. These Pyrenean examples provide an interesting stratigraphic and structural field analogue both in terms of basin architecture and oil prospectivity.

References

Alsop, G. I., R. Weinberger, T. Levi, and S. Marco (2015), Deformation within an exposed salt wall: Recumbent folding and extrusion of evaporites in the Dead Sea Basin, *J. Struct. Geol.*, *70*, 95–118.

Ardèvol, L., J. Klimowitz, J. Malagón, and P. J. Nagtegaal (2000), Depositional sequence response to foreland deformation in the Upper Cretaceous of the Southern Pyrenees, Spain, *AAPG Bull.*, *84*(4), 566–587.

Berástegui, X., J. M. García-Senz, and M. Losantos (1990), Tecto-sedimentary evolution of the Organyà extensional basin (central south Pyrenean unit, Spain) during the Lower Cretaceous, *Bull. Soc. Geol. Fr.*, *6*(2), 251–564.

Biteau, J.-J., A. L. Marrec, M. L. Vot, and J.-M. Masset (2006), The Aquitaine Basin, *Petrol. Geosci.*, *12*, 247–273.

Brinkmann, R. V., and H. Lögters (1968), Diapirs in Western Pyrenees and Foreland Spain, *Am. Assoc. Petrol. Geol. Mem.*, *8*, 275–292.

Brun, J. P., and X. Fort (2004), Compressional salt tectonics (Angolan margin), *Tectonophysics*, *382*(3–4), 129–150.

Butler, R. W. H., R. Maniscalco, G. Sturiale, and M. Grasso (2015), Stratigraphic variations control deformation patterns in evaporite basins: Messinian examples, onshore and offshore Sicily (Italy), *J. Geol. Soc.*, *172*(1), 113–124.

Callot, J. P., V. Trocmé, J. Letouzey, E. Albouy, S. Jahani, and S. Sherkati (2012), Pre-existing salt structures and the folding of the Zagros Mountains, *Geol. Soc. London, Spec. Publ.*, *363*, 545–561.

Callot, J. P., C. Ribes, C. Kergaravat, C. Bonnel, H. Temiz, A. Poisson, B. Vrielynck, J. F. Salel, and J. C. Ringenbach (2014), Salt tectonics in the Sivas basin (Turkey): Crossing salt walls and minibasins, *Bull. Soc. Geol. Fr.*, *185*(1), 33–42.

Calvet, F. (1986), El Triàsic, in *Història Natural dels Països Catalans*, vol. Geologia I, edited by P. Santanach, Enciclopedia Catalana, Barcelona.

Calvet, F., E. Anglada, and J. M. Salvany (2004), El Triásico de los Pirineos, in *Geología de España*, edited by J. A. Vera, pp. 272–274, SGE-IGME, Madrid.

Cámara, P. (1997), The Basque-Cantabrian basin's Mesozoic tectono-sedimentary evolution, *Mém. Soc. Géol. Fr.*, *171*, 187–191.

Canérot, J., M. R. Hudec, and K. Rockenbauch (2005), Mesozoic diapirism in the Pyrenean orogen: Salt tectonics on a transform plate boundary, *Am. Assoc. Pet. Geol. Bull.*, *89*(2), 211–229.

Caus, E., A. Gómez-Garrido, A. Simó, and K. Sofiano (1993), Cenomanian-Turonian platform to basin integrated stratigraphy in the South Pyrenees (Spain), *Cretaceous Res.*, *14*(4–5), 531–551.

Caus, E., A. Teixell, and J. M. Bernaus (1997), Depositional model of a Cenomanian-Turonian extensional basin (Sopeira Basin, NE Spain): Interplay between tectonics, eustasy and biological productivity, *Palaeogeogr. Palaeoclimatol. Palaeoecol.*, *129*(1–2), 23–36.

Cobbold, P. R., and P. Szatmari (1991), Radial gravitational gliding on passive margins, *Tectonophysics*, *188*(3–4), 249–289.

Courel, L., H. Aït Salem, N. Benaouiss, M. Et-Touhami, B. Fekirine, M. Oujidi, M. Soussi, and A. Tourani (2003), Mid-Triassic to Early Liassic clastic/evaporitic deposits over the Maghreb Platform, *Palaeogeogr. Palaeoclimatol. Palaeoecol.*, *196*(1–2), 157–176.

Déramond, J., P. Souquet, M. J. Fondecave-Wallez, and M. Specht (1993), Relationships between thrust tectonics and sequence stratigraphy surfaces in foredeeps: Model and examples from the Pyrenees (Cretaceous-Eocene, France, Spain), in *Tectonics and Seismic Sequence Stratigraphy*, edited by G. D. Williams and A. Dobb, *Geol. Soc. London, Spec. Publ.*, *71*, pp. 193–219.

Dooley, T. P., M. P. A. Jackson, and M. R. Hudec (2009), Inflation and deflation of deeply buried salt stocks during lateral shortening, *J. Struct. Geol.*, *31*(6), 582–600.

Dooley, T. P., M. P. A. Jackson, C. A. L. Jackson, M. R. Hudec, and C. R. Rodriguez (2015), Enigmatic structures within salt walls of the Santos Basin—Part 2: Mechanical explanation from physical modelling, *J. Struct. Geol.*, *75*, 163–187.

Drzewiecki, P. A., and J. A. Simo (1997), Carbonate platform drowning and oceanic anoxic events on a mid-Cretaceous carbonate platform, south-central Pyrenees Spain, *J. Sediment. Res.*, *67*(4), 698–714.

Drzewiecki, P. A., and J. A. Simo (2000), Tectonic, eustatic and environmental controls on mid-Cretaceous carbonate platform deposition, south-central Pyrenees Spain, *Sedimentology*, *47*, 471–495.

Drzewiecki, P. A., and J. A. Simó (2002), Depositional processes, triggering mechanisms, and sediment composition of carbonate gravity flow deposits: Examples from the Late Cretaceous of the south-central Pyrenees, Spain, *Sediment. Geol.*, *146*, 155–189.

Ferrer, O., E. Roca, B. Benjumea, J. A. Muñoz, N. Ellouz, and M. Team (2008), The deep seismic reflection MARCONI-3 profile: Role of extensional Mesozoic structure during the Pyrenean contractional deformation at the eastern part of the Bay of Biscay, *Mar. Pet. Geol.*, *25*, 714–730.

Ferrer, O., M. P. A. Jackson, E. Roca, and M. Rubinat (2012), Evolution of salt structures during extension and inversion of the Offshore Parentis Basin (Eastern Bay of Biscay), *Geol. Soc. London, Spec. Publ.*, *363*, 361–380.

Flinch, J. F., and J. M. Casas (1996), Inversion of a transfer system into lateral ramps: An example from the South-Central Pyrenees (Spain), *Geol. Rundsch.*, *85*, 372–379.

García Senz, J., and J. I. Ramirez (2016), Memoria y mapa geológico de España a escala 1:50.000 Hoja de Pont de Suert n°213 (32–10), Insituto Tecnológico y Geominero de España, Madrid, 2ª Serie MAGNA.

García Senz, J. M. (2002), Cuencas extensivas del Cretácico inferior en los Pirineos Centrales, formación y subsecuente inversión PhD thesis: Universitat de Barcelona, 294 p.

García-Mondéjar, J., L. M. Agirrezabala, A. Aranburu, P. A. Fernández-Mendiola, I. Gómez-Pérez, M. López-Horgue, and I. Rosales (1996), Aptian-Albian tectonic pattern of the Basque-Cantabrian Basin (northern Spain), *Geol. J.*, *31*, 13–45.

Garrido-Megías, A., and L. M. Ríos (1972), Síntesis geológica del Secundario y Terciario entre los ríos Cinca y Segre (Pirineo central de la vertiente surpirenaica, provincias de Huesca y Lérida), *Bol. Geol. Min. Esp.*, *83*(1), 1–47.

Gil, J. A. (1998), Modelización geodinámica y numérica de estructuras evaporíticas (cuencas surpirenaicas y cantábrica), PhD thesis, 200 pp., Universitat de Barcelona, Spain.

Giles, K. A., and M. G. Rowan (2012), Concepts in halokinetic-sequence deformation and stratigraphy, *Geol. Soc. London, Spec. Publ.*, *363*(1), 7–31.

Graham, R., M. Jackson, R. Pilcher, and B. Kilsdonk (2012), Allochthonous salt in the sub-Alpine fold-thrust belt of Haute Provence, France, *Geol. Soc. London, Spec. Publ.*, *363*(1), 595–615.

Harrison, J. C., and M. P. A. Jackson (2014), Exposed evaporite diapirs and minibasins above a canopy in central Sverdrup Basin, Axel Heiberg Island Arctic Canada, *Basin Res.*, *26*(4), 567–596.

Hearon, T. E., M. G. Rowan, T. F. Lawton, P. T. Hannah, and K. A. Giles (2014), Geology and tectonics of Neoproterozoic salt diapirs and salt sheets in the eastern Willouran Ranges South Australia, *Basin Res.*, *27*(2), 183–207.

Hudec, M. R., and M. P. A. Jackson (2007), Terra infirma: Understanding salt tectonics, *Earth Sci. Rev.*, *82*(1–2), 1–28.

Infoigme (2015a). [Available at http://info.igme.es/servicios/ServicioHidrocarburosSQL/Reports/Report.aspx?ReportName=ReportLinea&ReportParam=14378.]

Infoigme (2015b). [Available at http://info.igme.es/servicios/ServicioHidrocarburos/Reports/Report.aspx?ReportName=ReportLinea&ReportParam=14377.]

Infoterre-BRGM (2015). [Available at http://ficheinfoterre.brgm.fr/InfoterreFiche/ficheBss.action?id=10514X0012/BEL1.]

Jackson, C. A. L., M. P. A. Jackson, M. R. Hudec, and C. R. Rodriguez (2015), Enigmatic structures within salt walls of the Santos Basin—Part 1: Geometry and kinematics from 3D seismic reflection and well data, *J. Struct. Geol.*, *75*, 135–162.

Jackson, M. P. A., and B. C. Vendeville (1994), Regional extension as a geologic trigger for diapirism, *Geol. Soc. Am. Bull.*, *106*(1), 57–73.

Jackson, M. P. A., and C. J. Talbot (1992), A glossary of salt tectonics: Geological circular—Bureau of Economic Geology Univ. of Texas at Austin, v. 91-4.

Jackson, M. P. A., R. R. Cornelius, C. H. Craig, A. Gansser, J. Stocklin, and C. J. Talbot (1990), *Salt Diapirs of the Great Kavir, Central Iran*, *Memoir*, vol. 177, pp. 136, *Geol. Soc. Am.*, Boulder, Colo.

Jammes, S., G. Manatschal, L. Lavier, and E. Masini (2009), Tectonosedimentary evolution related to extreme crustal thinning ahead of a propagating ocean: Example of the western Pyrenees, *Tectonics*, *28*, TC4012, doi:10.1029/2008TC002406.

Jammes, S., G. Manatschal, and L. Lavier (2010a), Interaction between prerift salt and detachment faulting in hyperextended rift systems: The example of the Parentis and Mauléon basins (Bay of Biscay and western Pyrenees), *AAPG Bull.*, *94*(7), 957–975.

Jammes, S., C. Tiberi, and G. Manatschal (2010b), 3D architecture of a complex transcurrent rift system: The example of the Bay of Biscay-Western Pyrenees, *Tectonophysics*, *489*(1-4), 210–226.

Kennedy, W. J., and M. Bilotte (2014), Cenomanian ammonites from Santander (Cantabria) and Sopeira (Aragón, southcentral Pyrenees), northern Spain, *Treballs del Museu de Geol. de Barcelona*, *20*, 21–32.

Klimovitz, J., J. Malagón, S. Quesada, and A. Serrano (1999), Desarrollo y evolución de las estructuras salinas mesozoicas en la parte suroccidental de la CuencaVasco Cantábrica (Norte de España): Implicaciones exploratorias, in *Libro Homenaje a José Ramirez del Pozo*, edited by AGGEP, pp. 159–166.

Krzywiec, P. (2012), Mesozoic and Cenozoic evolution of salt structures within: The Polish Basin—An overview, *Geol. Soc. London, Spec. Publ.*, *363*, 381–394.

Lagabrielle, Y., P. Labaume, and M. de Saint Blanquat (2010), Mantle exhumation, crustal denudation, and gravity tectonics during Cretaceous rifting in the Pyrenean realm (SW Europe): Insights from the geological setting of the lherzolite bodies, *Tectonics*, *29*, TC4012, doi:10.1029/2009TC002588.

Lanaja, J. M., R. Querol, and A. Navarro (1987), *Contribución de la Exploración Petrolífera al Conocimiento de la Geología de España*, pp. 1–465, Instituto Geológico y Minero de España, Madrid.

Laubscher, H. P. (1977), Fold development in the Jura, *Tectonophysics*, *37*, 337–362.

Letouzey, J., B. Colletta, R. Vially, and J. C. Chermette (1995), Evolution of salt-related structures in compressional settings, in *AAPG Memoir 65 on Salt Tectonics: A Global Perspective*, vol. 65, edited by M. P. A. Jackson, D. G. Roberts, and S. Snelson, pp. 41–60, AAPG, Boulder, Colo.

López Olmedo, F., L. Ardèvol, P. P. Hernáiz, P. Cabra, J. Solé, J. Olivares, and F. Leyva (2016), Memoria y mapa geológico de España a escala 1:50.000 Hoja de Arén n° 251 (32-11), Insituto Tecnológico y Geominero de España, Madrid, 2ª Serie MAGNA.

Lopez-Mir, B., J. Anton Muñoz, and J. García Senz (2014a), Restoration of basins driven by extension and salt tectonics: Example from the Cotiella Basin in the central Pyrenees, *J. Struct. Geol.*, *69*, 147–162.

Lopez-Mir, B., J. A. Muñoz, and J. García-Senz (2014b), Extensional salt tectonics in the partially inverted Cotiella post-rift basin (south-central Pyrenees): Structure and evolution, *Int. J. Earth Sci.*, *104*(2), 419–434.

Manspeizer, W., J. Huntoon, R. Slingerland, K. Furlong, C. Beaumont, J. Diemer, and W. Newell (1989), Early Mesozoic rift basins of eastern North America: Origin and evolution, in *Sedimentology and Thermal Mechanical History of Basins in the Central Appalachian Orogen: Pittsburgh, Pennsylvania to Wallops Island, Virginia, July 1–8, 1989*, pp. 25–76, AGU, Washington, D. C.

Martínez, R. (1982), Distribución de los Ammonites del Cretácico sudpirenaico, *Cuad. Geol. Ibér.*, *8*, 1035–1047.

Martínez-Peña, B., and A. M. Casas Sainz (2003), Cretaceous-Tertiary tectonic inversion of the Cotiella Basin (southern Pyrenees, Spain), *Int. J. Earth Sci. (Geol Rundsch)*, *92*, 99–113.

Matias, H., P. Kress, P. Terrinha, W. Mohriak, P. T. L. Menezes, L. Matias, F. Santos, and F. Sandnes (2011), Salt tectonics in the western Gulf of Cadiz, southwest Iberia, *AAPG Bull.*, *95*(10), 1667–1698.

Maystrenko, Y. P., U. Bayer, and M. Scheck-Wenderoth (2012), Regional-scale structural role of Permian salt within the Central European Basin System, *Geol. Soc. London, Spec. Publ.*, *363*, 409–430.

McClay, K., J. A. Muñoz, and J. García-Senz (2004), Extensional salt tectonics in a contractional orogen: A newly identified tectonic event in the Spanish Pyrenees, *Geology*, *32*(9), 737–740.

Mey, P. H. W., J. C. Nagtegaal, K. J. Roberti, and J. A. Hartevelt (1968), Lithostratigraphic subdivision of post-Hercynian deposits in the south-central Pyrenees, Spain, *Leidse Geol. Mededelingen*, *41*, 221–228.

Michard, A., H. Ibouh, and A. Charrière (2011), Syncline-topped anticlinal ridges from the High Atlas: A Moroccan conundrum, and inspiring structures from the Syrian Arc Israel, *Terra Nova*, *23*(5), 314–323.

Moseley, F., J. C. Cuttell, E. W. Lange, D. Stevens, and J. R. Warbrick (1981), Alpine tectonics and diapiric structures in the Pre-Betic zone of southeast Spain, *J. Struct. Geol.*, *3*(3), 237–251.

Muñoz, J. A. (1992), Evolution of a continental collision belt: ECORS-Pyrenees crustal balanced section, in *Thrust Tectonics*, edited by K. R. McClay, pp. 235–246, Chapman and Hall, London.

Nagtegaal, P. J. C. (1972), Depositional history and clay minerals of the Upper Cretaceous basin in the south-central Pyrenees Spain, *Leidse Geol. Mededelingen*, *47*, 251–275.

Poprawski, Y., C. Basile, L. M. Agirrezabala, E. Jaillard, M. Gaudin, and T. Jacquin (2014), Sedimentary and structural record of the Albian growth of the Bakio salt diapir (the Basque Country, northern Spain), *Basin Res.*, doi:10.1111/bre.12062.

Puigdefàbregas, C., and P. Souquet (1986), Tectosedimentary cycles and depositional sequences of the Mesozoic and Tertiary from the Pyrenees, *Tectonophysics*, *129*, 173–203.

Puigdefàbregas, C., J. A. Muñoz, and J. Vergés (1992), Thrusting and foreland basin evolution in the Southern Pyrenees, in *Thrust Tectonics*, edited by K. R. McClay, pp. 247–254, Chapman and Hall.

Ringenbach, J., J. Salel, C. Kergaravat, C. Ribes, C. Bonnel, and J.-P. Callot (2013), Salt tectonics in the Sivas Basin Turkey: Outstanding seismic analogues from outcrops, *First Break*, *31*, 57–65.

Rios, J. (1948), Diapirismo, *Bol. Inst. Geol. Min. Esp.*, LX(20), 155–390.

Roca, E., J. A. Muñoz, O. Ferrer, and N. Ellouz (2011), The role of the Bay of Biscay Mesozoic extensional structure in the configuration of the Pyrenean orogen: Constraints from the MARCONI deep seismic reflection survey, *Tectonics*, 30, TC2001, doi:10.1029/2010TC002735.

Rosell, J. (1967), *Estudio geológico del sector del Prepirineo comprendido entre los ríos Segre y Noguera Ribagorzana (Prov. de Lérida): Pirineos*, vol. 21, pp. 214, Consejo Superior de Investigaciones Científicas, Madrid.

Rosell, J., and O. Riba (1966), *Nota sobre la disposición sedimentaria de los conglomerados de Pobla de Segur (Provincia de Lérida)*, pp. 3–16, Instituto de Estudios Pirenaicos, Zaragoza.

Rouby, D., S. Raillard, F. Guillocheau, R. Bouroullec, and T. Nalpas (2002), Kinematics of a growth fault/raft system on the West African margin using 3-D restoration, *J. Struct. Geol.*, 24(4), 783–796.

Rowan, M. G., and B. C. Vendeville (2006), Foldbelts with early salt withdrawal and diapirism: Physical model and examples from the northern Gulf of Mexico and the Flinders Ranges Australia, *Mar. Pet. Geol.*, 23(9–10), 871–891.

Rowan, M. G., T. F. Lawton, K. Giles, and R. Ratliff (2003), Near-salt deformation in La Popa basin, Mexico, and the northern Gulf of Mexico: A general model for passive diapirism, *AAPG Bull.*, 87(5), 733–756.

Rowan, M. G., K. A. Giles, T. E. Hearon, C. E. Gannaway, and J. C. Fiduk (2014), Megaflaps along the edges of steep diapirs and beneath salt sheets: Models and examples, in Proceedings AAPG International Conference & Exhibition, Istanbul, Turkey.

Salvany, J. M. (1990), Introducción a las evaporitas triásicas de las cadenas periféricas de la cuenca del Ebro: Catalánides, Pirineo y Región Cantábrica, in *Formaciones evaporíticas de la Cuenca del Ebro y cad. perifér., y de la zona de Levante*, edited by F. Ortí, pp. 9–20, Enresa, Madrid.

Samsó, J. M., J. García Senz, I. Mateos, J. J. Blázquez, A. Tallada, and R. Copons (2012a), El Pont de Suert 213-2-2, 1:25 000 Institut Geològic de Catalunya.

Samsó, J. M., J. García Senz, I. Mateos, A. Tallada, and R. Copons (2012b), Areny 251-2-1, 1:25 000 Institut Geològic de Catalunya.

Sannemann, D. (1968), Salt-stock families in northwestern Germany, in *Diapirism and Diapirs*, vol. 8, edited by J. Braunstein and G. D. O'Brien, pp. 261–270, AAPG Memoir, Boulder, Colo.

Saura, E. (2004), Anàlisi estructural de la zona de les Nogueres Pirineus Centrals.

Saura, E., and A. Teixell (2000), Relación entre los conglomerados oligocenos y las estructuras tectónicas en la zona de Les Nogueres Pirineo Central, *Geotemas*, 2, 201–203.

Saura, E., and A. Teixell (2006), Inversion of small basins: Effects on structural variations at the leading edge of the Axial Zone antiformal stack (Southern Pyrenees, Spain), *J. Struct. Geol.*, 28(11), 1909–1920.

Saura, E., et al. (2014), Syn- to post-rift diapirism and minibasins of the Central High Atlas (Morocco): The changing face of a mountain belt, *J. Geol. Soc.*, 171(1), 97–105.

Schultz Ela, D. D. (2003), Origin of drag folds bordering salt diapirs, *AAPG Bull.*, 87(5), 757–780.

Séguret, M. (1972), Étude tectonique des nappes et séries décollées de la partie centrale du versant sud des Pyrénées, Publication de l'Université de Sciences et Techniques de Languedoc, série Geologie Structurale, 2(2), 155 pp.

Serrano, A., and W. Martínez del Olmo (1990), Tectónica salina en el Dominio Cántabro-Navarro: Evolución, edad y origen de las estructuras salinas, in *Formaciones evaporíticas de la Cuenca del Ebro y cadenas periféricas, y de la zona de Levante*, edited by F. Ortí and J. M. Salvany, pp. 39–53, Enresa, Madrid.

Serrano, A., P. P. Hernaiz, J. Malagón, and C. Rodríguez Cañas (1994), Tectónica distensiva y halocinesis en el margen SO de la cuenca Vasco-Cantábrica, *Geogaceta*, 15, 131–134.

Shannon, P. M., and D. Naylor (1998), An assessment of Irish offshore basins and petroleum plays, *J. Pet. Geol.*, 21(2), 125–152.

Simó, A. (1985), Secuencias deposicionales del Cretacio superior de la Unidad del Montsec (Pirineo Central), PhD thesis, Universitat de Barcelona, Spain.

Simó, A., and C. Puigdefàbregas (1985), Transition from shelf to basin on an active slope, Upper Cretaceous, Tremp area, southern Pyrenees: Excursion Guide-book 6th European Regional Meeting Lérida, Spain, pp. 63-108.

Souquet, P. (1967), Le Crétacé supérieur sud-pyreneen en Catalogne, Aragon et Navarre, PhD thesis, Université de Toulouse, 529 p.

Teixell, A. (1996), The Ansó transect of the southern Pyrenees: Basement and cover thrust geometries, *J. Geol. Soc. Lond.*, 153, 301–310.

Teixell, A., and J. A. Muñoz (2000), Evolución tectono-sedimentaria del Pirineo meridional durante el Terciario: Una síntesis basada en la transversal del río Noguera Ribagorçana, *Revista Soc. Geol. Esp.*, 13(2), 251–264.

Tugend, J., G. Manatschal, and N. J. Kusznir (2015), Spatial and temporal evolution of hyperextended rift systems: Implication for the nature, kinematics, and timing of the Iberian-European plate boundary, *Geology*, 43(1), 15–18.

van Hoorn, B. (1970), Sedimentology and paleogeography of an Upper Cretaceous turbidite basin in the south-central Pyrenees Spain, *Leidse Geol. Mededelingen*, 45, 73–154.

Vargas-Meleza, L., D. Healy, G. I. Alsop, and N. E. Timms (2015), Exploring the relative contribution of mineralogy and CPO to the seismic velocity anisotropy of evaporites, *J. Struct. Geol.*, 70, 39–55.

Vergés, J. (1993), Estudi geològic del vessant Sud del Pirineu Oriental i Central: Evolució en 3D, PhD thesis, 203 pp., Universitat de Barcelona, Spain.

Vergés, J., and A. Martinez (1988), Corte compensado del Pirineo oriental Geometría de las cuencas de antepaís y edades de emplazamiento de los mantos de corrimiento, *Acta Geol. Hisp.*, 23, 95–106.

Vergés, J., and J. M. García Senz (2001), Mesozoic evolution and Cenozoic inversion of the Pyrenean rift, in *Peri-Tethys Memoir 6: Pery-Tethyan Rift/Wrench Basins and Passive Margins*, vol. 186, edited by P. A. Ziegler et al., pp. 187–212, Mémoires Muséum National d'Histore Naturelle, Paris.

Vergés, J., H. Millán, E. Roca, J. Muñoz, M. Marzo, J. Cirés, T. den Bezemer, R. Zoetemeijer, and S. Cloetingh (1995), Eastern Pyrenees and related foreland basins: Pre-, syn- and post-collisional crustal-scale cross-sections, *Mar. Pet. Geol.*, 12(8), pp. 903–915, doi:10.1016/0264-8172(95)98854-X.

Wagner, G., F. Mauthe, and H. Mensink (1971), Der Salzstock von Cardona in Nordospanien, *Geol. Rundsch.*, 60(3), 970–996.

Warren, J. K. (2010), Evaporites through time: Tectonic, climatic and eustatic controls in marine and nonmarine deposits, *Earth Sci. Rev.*, 98(3–4), 217–268.

Ziegler, P. A. (1989), Geodynamic model for Alpine intra-plate compressional deformation in Western and Central Europe, in *Inversion Tectonics*, edited by M. A. Cooper and G. D. Williams, *Geol. Soc. London, Spec. Pub.*, pp. 63–85.